CHALMERS
UNIVERSITY OF TECHNOLOGY

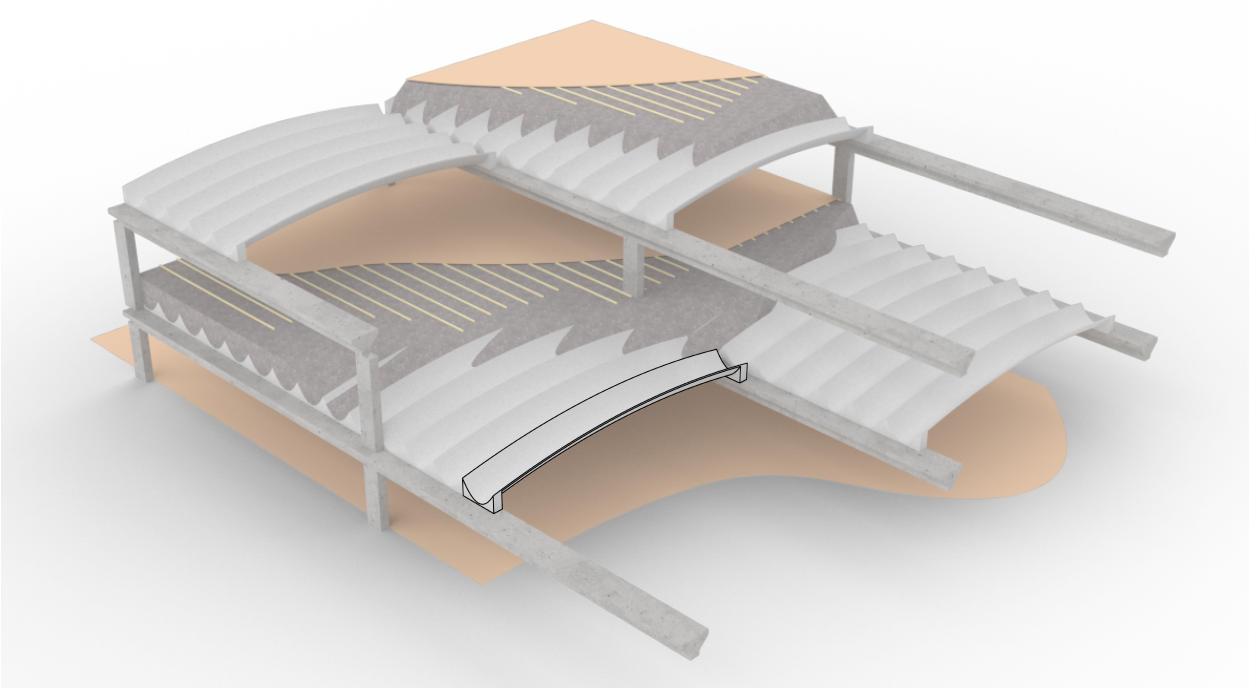

Design and evaluation of doubly-curved shell-like concrete slab elements

Pre-stressed structurally optimized elements and their potential to reduce the climate impact

Master's thesis in Master Program Design and Construction Project Management

ERIK ARLINGER

Division of Construction Management at Chalmers
CHALMERS UNIVERSITY OF TECHNOLOGY
Master's thesis ACEX30
Gothenburg, Sweden 2023

Master's thesis ACEX30

Design and evaluation of doubly-curved shell-like concrete slab elements

Pre-stressed structurally optimized elements and their potential to reduce the climate impact

ERIK ARLINGER

CHALMERS
UNIVERSITY OF TECHNOLOGY

Department of Architecture and Civil Engineering
Division of Construction Management at Chalmers
Chalmers University of Technology
Gothenburg, Sweden 2018

Design and evaluation of doubly-curved shell-like concrete slab elements
Pre-stressed structurally optimized elements and their potential to reduce the climate impact

ERIK ARLINGER

Supervisor: PhD Alexander Sehlström, Lead Structural Engineer, Property & Buildings, WSP
Examiner: Research engineer Mikael Johansson, Department of Architecture and Civil Engineering

Department of Architecture and Civil Engineering
Division of Construction Management
Chalmers University of Technology
SE-412 96 Gothenburg
Telephone +46 31 772 1000

Cover: Thought slab system, where a slab element is highlighted with black. The system is filled to achieve a level top, on which interior floor is placed (see fig. 1.1).

Division of Construction Management at Chalmers
Gothenburg, Sweden 2018

Design and evaluation of doubly-curved shell-like concrete slab elements
Pre-stressed structurally optimized elements and their potential to reduce the climate impact
Erik Arlinger
Department of Construction Management
Chalmers University of Technology

Abstract

The climate impact of the construction sector must reduce to meet the Paris agreement. Horizontal concrete elements make up for a large share of the sector's impact. This thesis explores doubly-curved shell-like concrete elements and their potential to reduce concrete usage of the sector. The element is explored through design and finite element analysis.

The design process starts off with a primary design study of three different slab elements. The geometry is evaluated, and the result is brought into the next study. In the second study, pre-stress, fill and geometrical adaptations are introduced. One slab element is found to have a beneficial structural behaviour. This element is brought to the last design study, where the behaviour of the element is further explored. The element behavior gave the idea for a final pre-stressing case, where the tensile stresses in the slab are reduced enough to be handled by the concrete material. In the 4th and last study, the production and climate impact of the final slab is discussed.

The production method derives from some geometrical properties found in the design studies, and the production is realistic. The material climate impact of the final doubly-curved shell-like slab is found to be 30% of the material climate impact for slabs common today.

Keywords: Structural optimization, Concrete shells, Ruled surface, Form-found surface, Pre-stress, Material efficiency

Acknowledgements

This thesis would not have been possible without my supervisor Alexander Sehlström at WSP Gothenburg. Alexander came up with the idea of the subject, and guided me with a steady hand. His insights, knowledge and structural expertise has been vital for the thesis. He has also been a rock during doubting hours. Thank you Alexander. Thanks also to Karl-Gunnar Olsson, Rasmus Rempling and Johan Lagerkvist at Chalmers and Trafikverket for input during and after the make-shift seminar. Thank you to Strusoft and Andreas Oscarsson for giving me a hand when I needed further guidance in FEM-design and the Grasshopper API. Also a thank you to my examiner, Mikael Johansson, for great input and many laughts. A special thanks to Lisa, for putting up with my late nights and talk of concrete. I love you.

Preface

I have a bachelor in Architecture and Engineering from Chalmers University of Technology, and through this a great interest for structural behavior and efficiency. This thesis is written as a part of the Design and Construction Project Management masters program at Chalmers. Because of these two fields, this thesis is written with one foot in each camp, trying to improve the construction sector through structural optimization.

Erik Arlinger, Gothenburg, June 2023

Contents

List of Figures

List of Tables

1

Introduction

To fulfill the aris agreement, the global construction sector need to be net-zero carbon by 2050 (United Nations Environment Programme, 2022). This requires the emissions from the construction and operation of buildings to be reduced by 98% from 2020, with all new buildings being net-zero carbon by 2030. The large drop in emissions from the construction sector in 2020 caused by the Covid-19 pandemic was rebounded by 2021 in most major economies. The Global Buildings Climate Tracker IEA (2022a) shows that the recent actions taken by the industry (for example, the development of national building energy codes, high-performing building envelopes, and more efficient indoor climate systems) are not near good enough to keep the reduction in pace with the path required to reach the goal.

The production of concrete makes up 7% of the annual global carbon emissions (GlobalABC et al., 2020). To get on track with the net-zero by 2050 scenario, the emissions of the global cement production must be reduced by 10% in 2030 (IEA, 2022a). The reduction might be achieved by the use of sustainably produced and sourced concrete, but the development is slow, and the green concrete does not eliminate the climate impact, and is an expensive alternative (IEA, 2022b). Another possibility is to reduce the material use (GlobalABC et al., 2020). Since the built floor area is predicted to increase by 2% per year until 2030 (IEA, 2022a), we need to reduce the concrete use by increasing the structural efficiency of our building elements. This would lower the amount of material needed to produce buildings, while maintaining the structural strength.

The horizontal concrete building elements, such as slabs and beams, are the single largest contributor towards the environmental impact of tall building structures (20-70 stories), and makes up 57-82% of the embodied energy of these (Foraboschi et al., 2014). The geometry of concrete slabs used today is not optimal. A certain slab height is required to handle the bending moment in the middle of the span. Some improvements to horizontal elements has been done, like pre-stressed reinforcement and reduction of material in the middle of the slab height. However, the bending moment still limits the reduction of material. Development of the geometry of concrete slabs could greatly reduce the bending moment, thereby reducing the amount of material needed to support the same load. One shape that could be the solution is the *doubly-curved shell*, which has a different structural behaviour compared to the flat slabs used today (Dombrowski et al., 2021).

1.1 Aim

This thesis aim to explore the possibility to reduce the climate impact by improving the structural efficiency of horizontal concrete elements through shell-like slab geometry.

The work departs from this hypothesis:

The doubly-curved shell-like shape is possible to use as thin pre-cast concrete slab elements. The shape is adapted to fit the current application of conventional horizontal concrete slabs by limiting the tensile forces through geometry design and pre-stressing. The thin doubly-curved slab has the potential to reduce usage of concrete in the construction sector, resulting in a reduced climate impact. The slab can replace the hollow core slabs commonly used today, working as a closed slab system on which interior floor can be placed, see fig. 1.1. Another possible application is as bridge deck elements.

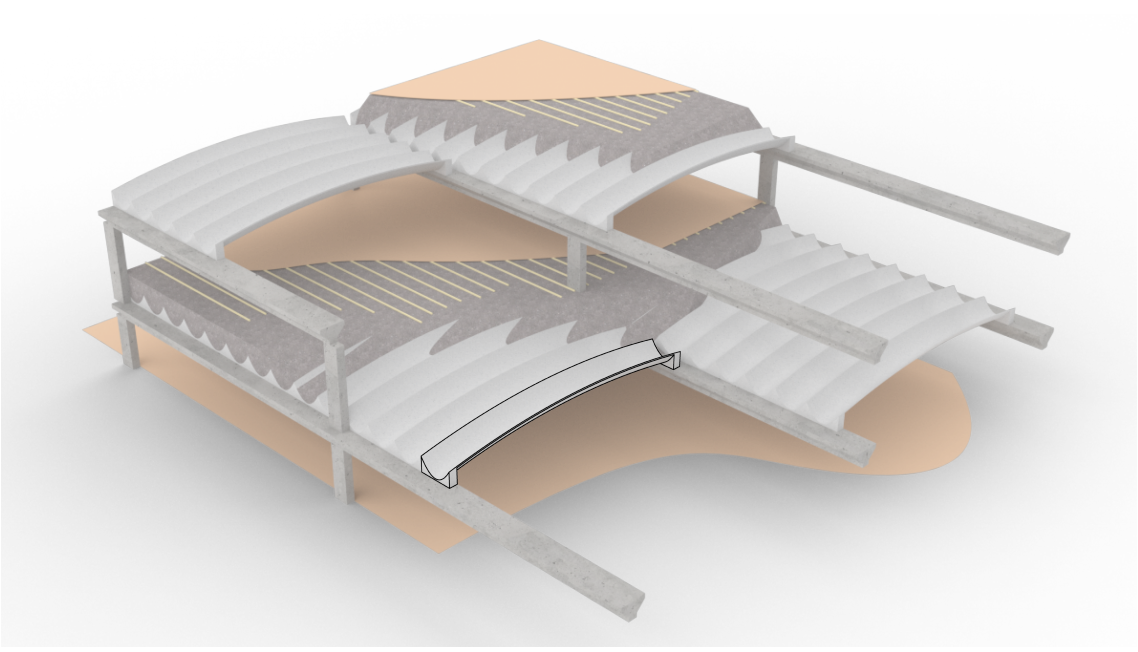

Figure 1.1: *Thought slab system, where a slab element is highlighted with black. The system is filled to achieve a level top, on which interior floor is placed.*

1.2 Scope & Limitations

The width of pre-fabricated concrete slabs used in Swedish buildings today is 1200 mm (Svensk betong, 2015), which will also be the set width of the slabs handled by this thesis. The length that will be studied is 10 m.

The software used to run the structural analysis require flat surfaces, and cannot handle curved meshes or NURBS. To make the analysis effective, the model of the slab was approximated by 340 flat surfaces.

1.3 Objectives

To understand how doubly-curved concrete slabs could improve the efficiency of horizontal construction elements and reduce material usage in the construction industry, this thesis has the following objectives:

- To explore and describe design choices that affects the structural efficiency in concrete slabs.
- To design and evaluate a doubly-curved slab element, to a point where it is theoretically implementable.
- To compare the resulting design with currently used systems, to see if the new slab element can reduce the climate impact.

2

Background

2.1 Shells and their application in architecture

According to Williams Williams (2014), a *shell* is defind as:

> A shell is a structure defined by a curved surface. It is thin in the direction perpendicular to the surface, but there is no absolute rule as to how thin it has to be.

The definition could be applied to many tensile structures, but the term is most common to describe rigid structures.

The term shell is broad and refers to many objects and shapes. The shape is often found in nature, like in eggs or clams. The egg is a *closed shell*, while the clam is an *open shell*. In architecture, the term often refers to larger essentially horizontal structures that are used either as a supporting structure, like in stone cathedrals, for example, the Church of Colònia Güell by Antoni Gaudí fig. 2.2, or as the entire building envelope, like in Oceanogràfic València (fig. 2.1). The structure can be complex or simple, light or heavy, made up by one entire shell or including multiple 'sub' shells. One of the most famous shell structures of today is the Sidney Opera House (fig. 2.3a), by Jørn Utzon.

Figure 2.1: *Oceanogràfic València.*

Figure 2.2: *Church of Colònia Güell.*

The usage of shell-like structures to make big-span roofs has been around for millennia, with examples like the still standing Pantheon in Rome (fig. 2.3b). The discovery of the optimal shape for compressive forces is credited to Robert Hooke, who in 1676 published ten 'inventions', with the third invention being the law for elasticity, today called *Hooke's Law*. His description for the path of compressive forces translated to English states "As hangs the flexible line, so but inverted will stand the rigid arch" (Ochsendorf & Block, 2014).

(a) *Sidney Opera House.*

(b) *Ceiling of the Pantheon in Rome.*

Figure 2.3: *Two shell structures, built ca 1800 years apart. The opera house consist in multiple smaller sub-shells, while the pantheon ceiling is constructed as one large shell-like dome with a circular hole in the middle. The purpose of the hole (the oculus) was either structural and/or to allow daylight inside.*

2.1.1 Doubly-curved geometry

The term doubly-curved refers to geometry that is curved in two directions of a surface. The arch, the cylinder and the cone are examples of single-curved geometries (see fig. 2.4). The hyperboloid, the sphere and the egg are examples of doubly-curved geometries (see fig. 2.5).

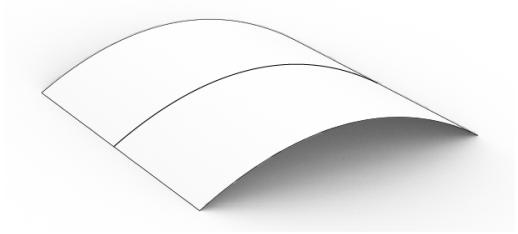

Figure 2.4: *Single-curved surface.*

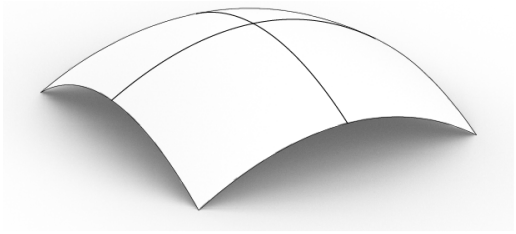

Figure 2.5: *Dounly-curved surface.*

2.2 Pre-cast concrete

The process of pre-casting concrete has been around since the industrial revolution, but the industrialized custom pre-fabrication of elements used today was developed around 1970-2000 (Elliot, 2017). Instead of building forms on site which are then

torn down after the concrete curing, the pre-fab production uses the same mould many times to create modules delivered to the construction site on schedule. This allows a quicker construction process due to the elimination of the concrete hardening time on site. The literature is in agreement that the pre-fabricated elements not only saves time during the construction process, but is also limits the waste arising from the form-work and concrete works by 51–87% (Jaillon, Poon, & Chiang, 2009). Two examples of pre fabricated slab elements commonly used today is the hollow core slab, fig. 2.6, and the TT slab, fig. 2.7.

Figure 2.6: *Hollow core slab. Photo credit: Elematic.*

Figure 2.7: *TT slab. Photo credit: Elematic.*

3
Methodology

This thesis is centred around four studies, each one representing one step of the iterative design process. The iterative design approach is chosen to best utilize the lessons learned throughout the thesis process. The first 3 studies are design oriented, and aim to conclude a realistic design that could be implemented in the construction industry. The 4th study revolves around evaluation of the results and discussions from the first 3 studies. The studies are divided as:

- **Study I** Primary design and evaluation of doubly-curved concrete slabs
- **Study II** Further Adaptation and pre-stressing of the ruled surface slab
- **Study III** Structure elaboration
- **Study IV** Production and climate impact

Each study includes method, results, and discussion. Figure 3.1 illustrates the thesis chapter structure, where Introduction, Background and Theory leads in to Study I. Studies II and III makes up the focal point of the slab element design, which is then evaluated and discussed in Study IV and the Discussion and conclusions chapter.

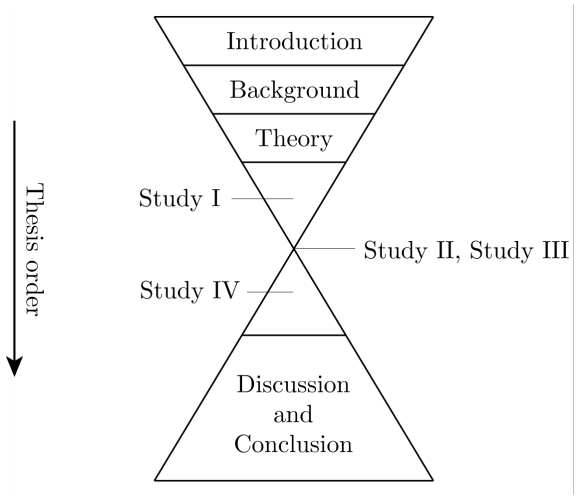

Figure 3.1: *Thesis chapter structure.*

The chapters Introduction, Background, and Theory are based on a broad literature study, where climate impact of construction was mixed with theory of structural efficiency.

3.1 Software

The generation of structural analysis models was conducted in Grasshopper, a visual programming environment inside the Rhinoceros 3D CAD software (Robert McNeel & Associates, 2022). In Grasshopper geometry is created by defining and changing parameters with “components”.

For finite element analysis, the FEM-Design 3D structures by Strusoft (2023a) was used. The grasshopper model was mounted to the FEM software using the FEM-Design API (2023b).

4

Theory

4.1 Geometrical definitions

This section describes the two geometrical definitions used in this thesis: ruled surfaces and form-found surfaces.

4.1.1 Ruled surfaces

Ruled surfaces are defined by a continuous family of straight lines called *generatrices*(Osman-Letelier et al., 2019). The generatrices of one dimension is originating from the same continuous curve, so called *directrix*. Examples of ruled surfaces are cylinders, cones , hyperboloids and hyperbolic paraboloids (see fig. 4.1).

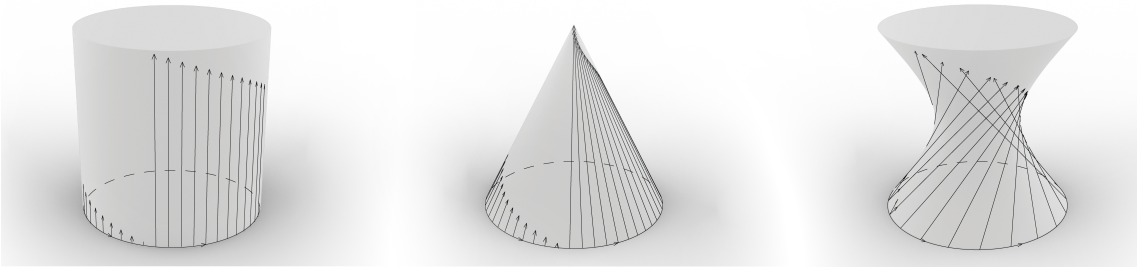

Figure 4.1: *A cylinder, a cone and a hyperboloid.*

4.1.2 Form-found surfaces

The form-finding process is different from the ruled surface, where the form is found by letting gravity interact with the structural behaviour of the material, thereby resulting in a naturally formed bending-free shape. The method was first mentioned by Hooke (see section 2.1), and can be translated as: The inverted shape of a tensile hanging structure is the optimal one for a standing structure carrying loads by compression (see fig. 4.2). The supports needs to have the same placement and behaviour (for the xy-plane, inverted for the z-direction) in the two structures.

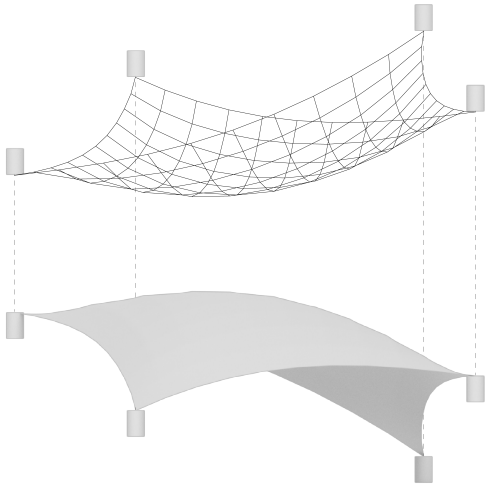

Figure 4.2: *Hanging tensile structure, with its inverse carrying compression.*

4.2 Load combinations

In Eurocode there are multiple load combinations defined, describing which load cases to include and what factor to multiply these with for each load combinations depending on load period and expected load size. Table 4.1 lists the load combinations used in this thesis.

Table 4.1: *Load combinations used, where U stands for ultimate. Sc, Sf and Sq are different serviceability limit states.*

Load combination		**Partial factor γ**	**Characteristic load**
STR 6.10a	U	1.35 1.35	Dead load Dead load fill
STR 6.10b Live load whole	U	1.2 1.2 1.5	Dead load Dead load fill Live load whole
STR 6.10b Live load half	U	1.2 1.2 1.5	Dead load Dead load fill Live load half
SLS 6.14b Live load	Sc	1 1 1	Dead load Dead load fill Live load
SLS 6.15b Live load	Sf	1 1 0.5	Dead load Dead load fill Live load
SLS 6.16b Live load	Sq	1 1 0.3	Dead load Dead load fill Live load

4.3 Material properties

This section discusses relevant properties of material, such as concrete and pre-tension steel.

4.3.1 Concrete

The material properties of this thesis are retrieved from Eurocode (2023). According to Eurocode 2 (EC 2) the design compressive strength is calculated as

$$f_{cd} = \alpha_{cc} \frac{f_{ck}}{\gamma_c}, \tag{4.1}$$

where α_{cc} is a coefficient taking account of long term effects on the compressive strength and of unfavourable effects resulting from the way the load is applied, γ_c is the partial safety factor for concrete ($= 1.5$), and f_{ck} is the characteristic cylinder compressive strength. Table 4.2 lists f_{ck} and f_{cd} for some common concrete strength classes.

Table 4.2: *Characteristic cylinder compressive strength f_{ck} and design compressive strength f_{cd} for α_{cc} = 1.00 for the concrete classes described in EC 2.*

class	12/15	16/20	20/25	25/30	30/37	35/45	40/50
f_{ck} [MPa]	12	16	20	25	30	35	40
f_{cd} [MPa]	8.00	10.67	13.33	16.67	20.00	23.33	26.67

class	45/55	50/60	55/67	60/75	70/85	80/95	90/105
f_{ck} [MPa]	45	50	55	60	70	80	90
f_{cd} [MPa]	30.00	33.33	36.67	40.00	46.67	53.33	60.00

According to EC 2 the design tensile strength is calculated as

$$f_{ctd} = \alpha_{ct} \frac{f_{ctk0,05}}{\gamma_c}, \tag{4.2}$$

where α_{ct} is a coefficient taking account of long term effects on the tensile strength and of unfavourable effects resulting from the way the load is applied and $f_{ctk0,05}$ is the characteristic tensile strength. Table 4.3 lists $f_{ctk0,05}$ and f_{ctd} for some common concrete strength classes.

Table 4.3: *Characteristic tensile strength $f_{ctk0,05}$ and design tensile strength f_{ctd} for α_{ct} = 1.00 for the concrete classes described in EC 2.*

class	12/15	16/20	20/25	25/30	30/37	35/45	40/50
$f_{ctk0,05}$ [MPa]	1.1	1.3	1.5	1.8	2.0	2.2	2.5
f_{ctd} [MPa]	0.73	0.89	1.03	1.20	1.35	1.50	1.64

class	45/55	50/60	55/67	60/75	70/85	80/95	90/105
$f_{ctk0,05}$ [MPa]	2.7	2.9	3.0	3.1	3.2	3.4	3.5
f_{ctd} [MPa]	1.77	1.90	1.97	2.03	2.15	2.26	2.35

4.3.1.1 Climate Impact of Concrete

The resulting geometry of this thesis will be compared to 2 different concrete slab systems presented by Högström and Olsson (2001). This is done to evaluate the climate impact of the resulting slab. The data for material climate impact is retrieved from Boverket's climate database for the life cycle phases A1-A3 (conservative value).

4.3.2 Pre-stressing

To improve the performance of structures carrying forces through compression, pre-stressing is a method commonly used. Sehlström (2021) discusses this and its applications used today. The method is based on the idea of adjusting the structural behavior of an object by applying forces that counter stresses or movement to the object. An example is the spokes in a bicycle wheel, that without pre-stress would wobble and ultimately not work.

The Swedish Standard Institute has as an addition to Eurocode 2 giving specific properties for high tensile steel wire strands in SS 212553 (2013). All pre-stressing strands used in this thesis is of class Strand SS 212553-Y1860S7 with a yield strength of 1860 MPa.

4.4 Structural terminology

Loading any object give rise to a state of stress within the object. For thin shells, the state of stress is dominated by membrane stresses acting in the tangent plane of the shell. At any point on the shell, the membrane stresses can be expressed in terms of its normal and shear stress components σ_X, σ_Y, $\tau_{XY} = \tau_{YX}$ relative to an arbitrary orthogonal coordinate system with axes denoted X and Y (fig. 4.3, left). By rotating the coordinate system an angle θ_p around the surface normal such that the shear stresses components vanish, the state of stress can be expressed in terms of its *principal stresses* σ_1 and σ_2 (Timoshenko & Goodier, 1951) (fig. 4.3, right). These act along the orthogonal *principal directions*, which, in general, are different at every point on the shell.

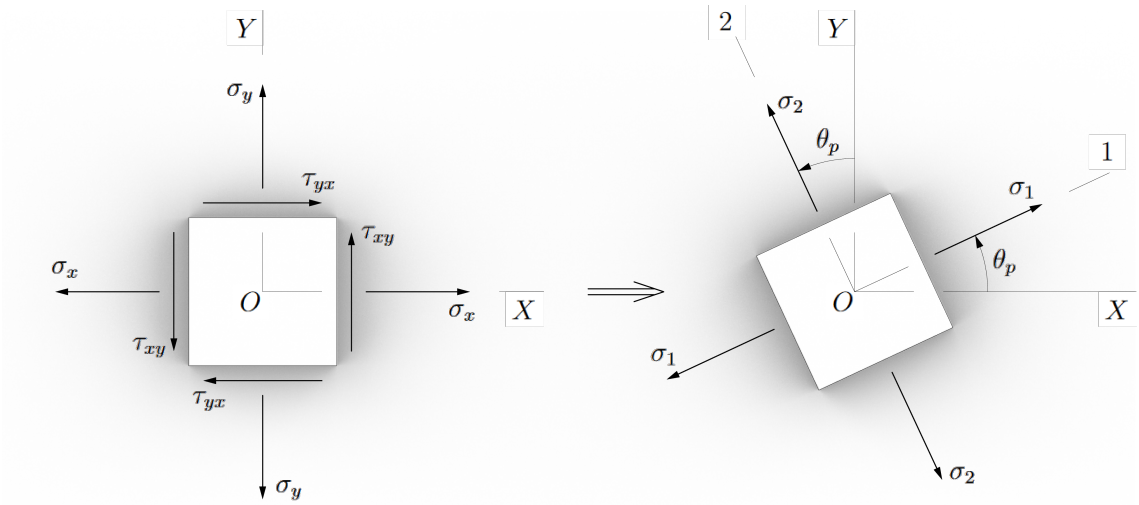

Figure 4.3: *Stresses in given coordinate system, translated to principal stresses.*

For the stress plots, the negative (compressive) stresses are drawn in red, and the positive (tensile) stresses are drawn in blue.

5

Study I

Primary design and evaluation of doubly-curved concrete slabs

Study I aims to lay the basis for the design and evaluation of the doubly-curved shell-like slab. A first iteration of design will be made, and the outcomes of the evaluation for this design will be the starting point for Study II. The questions that Study I aims to answer is:

- How does different geometries behave when loaded?
- Can any geometries be discarded?
- How does the support type affect the structural behaviour of the slab?
- Can the doubly-curved geometry provide a efficient and stiff enough solution to compete with the slabs used in the construction industry today?

There are three different geometries generated in Study I, one ruled where the dimensions and shape of the slab is specifically defined (see section 4.1.1) and two form-found surfaces, a concave and and a convex (see section 4.1.2).

The slab height was set to 1 m for the ruled surface. The form-found surfaces were designed to receive similar height.

5.1 Method

In this section the three processes making up Study I will be described as follows: model generation (geometry, loads and supports), analysis and evaluation.

5.1.1 Model generation

5.1.1.1 Ruled surface

Figure 5.1 illustrates the step-wise generation of the ruled surface model. To achieve a doubly-curved slab, two sets of directrices were generated. The dimensions of the slab were defined by the domain of the first directrix (fig. 5.1a), which was then mirrored twice, by the yz- and xz-planes (fig. 5.1b). Each directrix was then divided into an even number of parts with equal length (fig. 5.1c). The number of divided parts determined the mesh complexity, where more parts increased the precision of the shape approximation at the cost of increased computational demand. Two sets of generatrices were then placed between the points on the opposing directrices, creating a grid (fig. 5.1d). The grid was then triangulated and divided into the

desired slab shape by an extruded rectangle with one corner in the midpoint of each directix (fig. 5.1e). Since the shape was generated by four symmetric lines, the length and width of the resulting slab was equal to the x- and y- domain of the first directrix. The shape height equals 1/4 of the directrix z-domain.

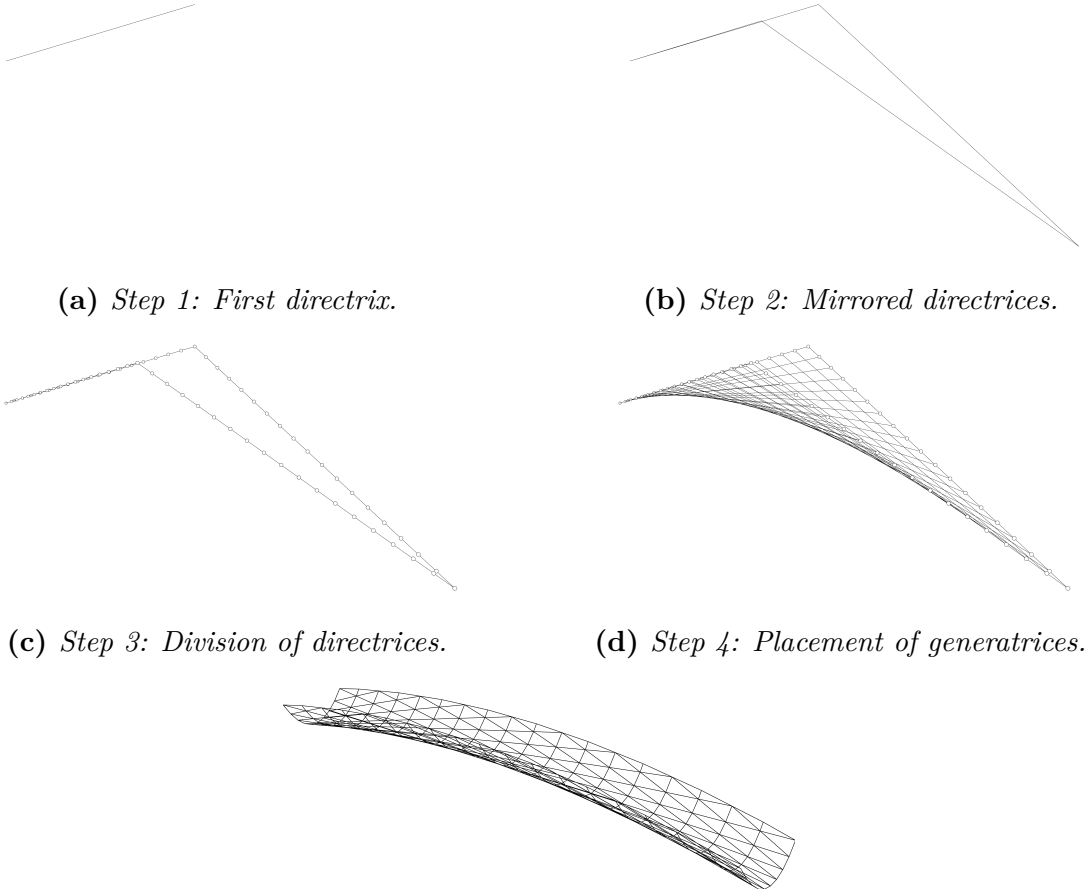

(a) *Step 1: First directrix.*

(b) *Step 2: Mirrored directrices.*

(c) *Step 3: Division of directrices.*

(d) *Step 4: Placement of generatrices.*

(e) *Step 5: Splitting of mesh and triangulation.*

Figure 5.1: *Generation of ruled geometry.*

5.1.1.2 Form-found surfaces

Figure 5.2 illustrates the step-wise generation of the form-found models. The form-found surfaces were started out in the same way as the ruled surfaces in order to generate a similar adjustable mesh. Instead of three-dimensional directrices, the surface was defined in the xy-plane (fig. 5.2a) and then 'hung' using the physics engine Kangaroo2 (Piker, 2017) in Grasshopper. The yz-section of the slab was first formed by fixating the edges along the x-direction, and the edges along the y-axis to the yz-plane. The interior mesh edges were then defined as springs and a uniform load was applied at each vertex of the mesh. The resulting single-curved mesh (fig. 5.2b) formed the basis for both the *concave* and the *convex* form-found surfaces.

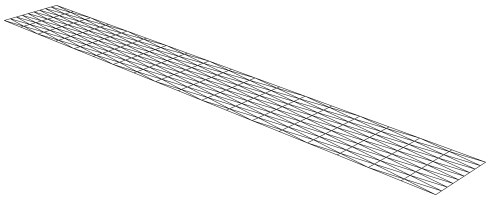

(a) *Step 1: mesh generation in xy-plane.*

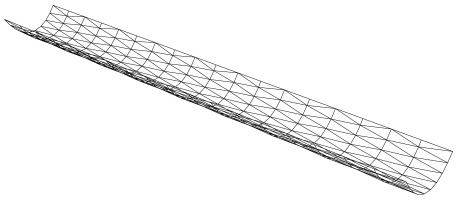

(b) *Step 2: generation of basis.*

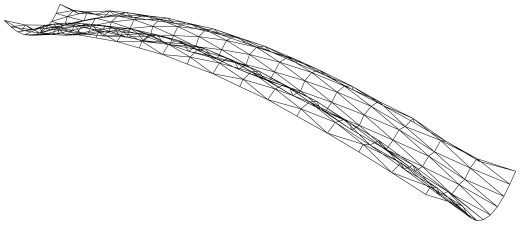

(c) *Step 3a: generation of concave shape.*

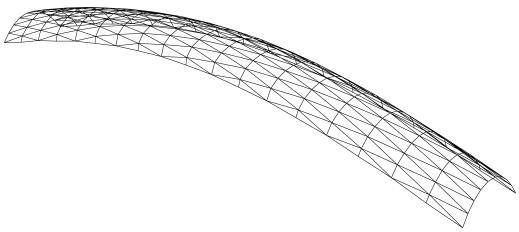

(d) *Step 3b: generation of convex shape.*

Figure 5.2: *Generation of form-found slab geometry.*

The curved edges were then fixed, and the old straight supported edges were fixed to the xz-plane, allowing them to move along the x- and z-axis. The same load was applied, in the same direction as before for the concave (fig. 5.2c) and opposite direction for the convex (fig. 5.2d). The z dimensions (height) of the resulting shapes were determined by load magnitude or spring strength.

5.1.1.3 Load generation

Three different loads were generated, one simulating gravel filling to adjust the upper level of the slab system, and two different surface loads. One surface load covered the entire slab and the other only half, both with magnitude 2.5 kN/m^2 (fig. 5.3). Since load combination SRT 6.10b (see table 4.1) give rise to the largest load effect, therefore this load combination was used for analysis of the models.

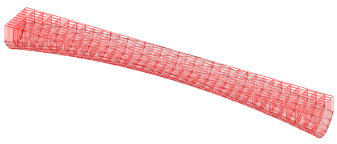

(a) *Dead load, gravel fill.*

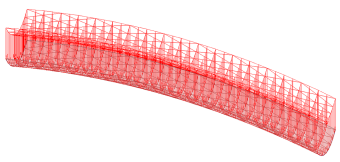

(b) *Live load, whole.*

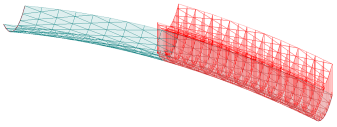

(c) *Live load, half.*

Figure 5.3: *The tree load cases, gravel fill, surface whole and surface half.*

5.1.1.4 Support generation

The exterior edges along the y-axis were modelled as linear supports, with the curvature divided into straight lines along the flat surface edges. Two different support setups were studied for each slab, one making the slab *simply-supported* with supports only handling forces in z-direction, one *hinged* where the supports is fixed in space but can rotate freely (fig. 5.4).

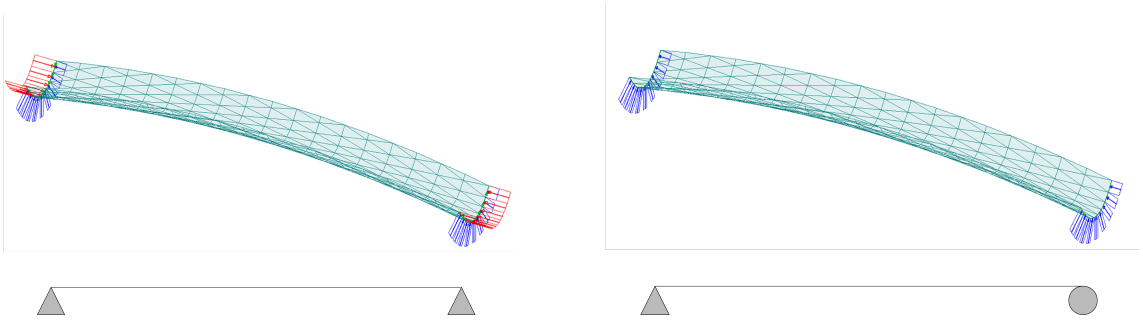

(a) *Hinged support.* **(b)** *Simply-supported.*

Figure 5.4: *The two support types, hinged and simply-supported.*

5.1.2 Model analysis

The geometry generated was mounted to a FEM-design 3D Structures model (Strusoft, 2023a) using the FEM-Design API (Strusoft, 2023b) for Grasshopper. The flat faces of the generated meshes were converted into surfaces, and modelled as 5 cm thick plates in FEM-design. No reinforcement was used in this study. The material decided was concrete class C12/15.

5.1.3 Model evaluation

The analysis resulted in one model for each slab with the two support types. From the models, all forces, stresses, and deflections were obtainable. The ones decided as relevant were taken out and put into tables. These were:

- principal stresses,
- stress patterns,
- maximum compression ($\sigma_{c,\max}$) and maximum tension ($\sigma_{t,\max}$),
- stresses in the slab centre (σ_{centre}) and at the edge of the slab middle section (σ_{mid}),
- maximum deflection $\delta_{\max}$.

To further understand how the different slabs behaves with the two supports, the principal stresses were plotted against the slab geometries.

5.2 Results

The results for Study I consists in final model geometry (fig. 5.5), stresses and deformations (table 5.1) and plotted principal stresses (fig. 5.6). The principal stress plot shows stress directions and magnitude with lines in blue for tension and red for compression. The line length represents the stress magnitude.

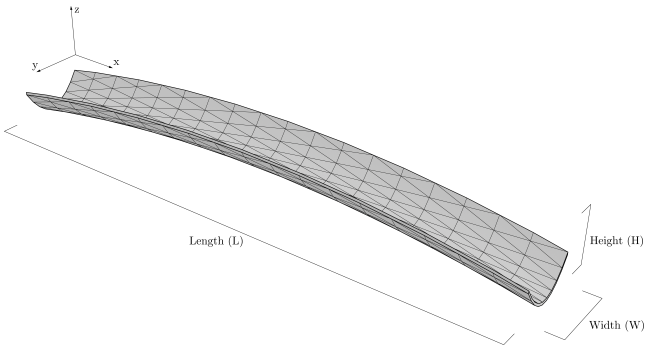

(a) *Ruled geometry.*

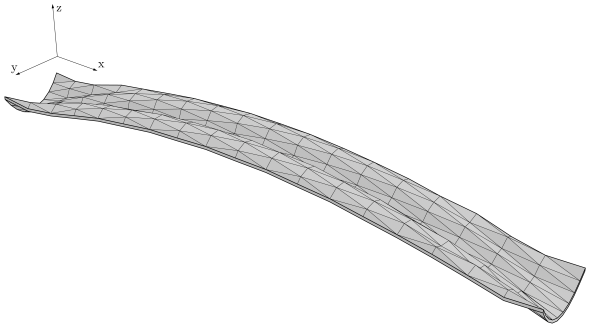

(b) *Concave form-found geometry.*

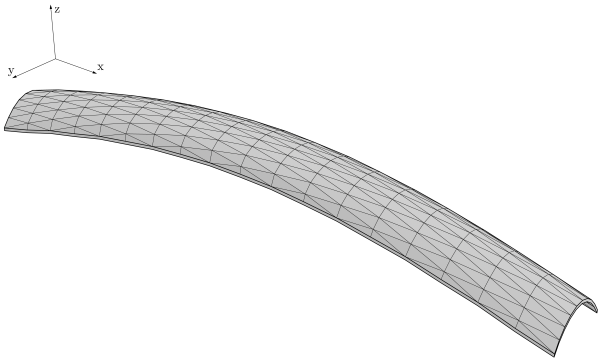

(c) *Convex form-found geometry.*

Figure 5.5: *Generated geometry used in calculation and evaluation.*

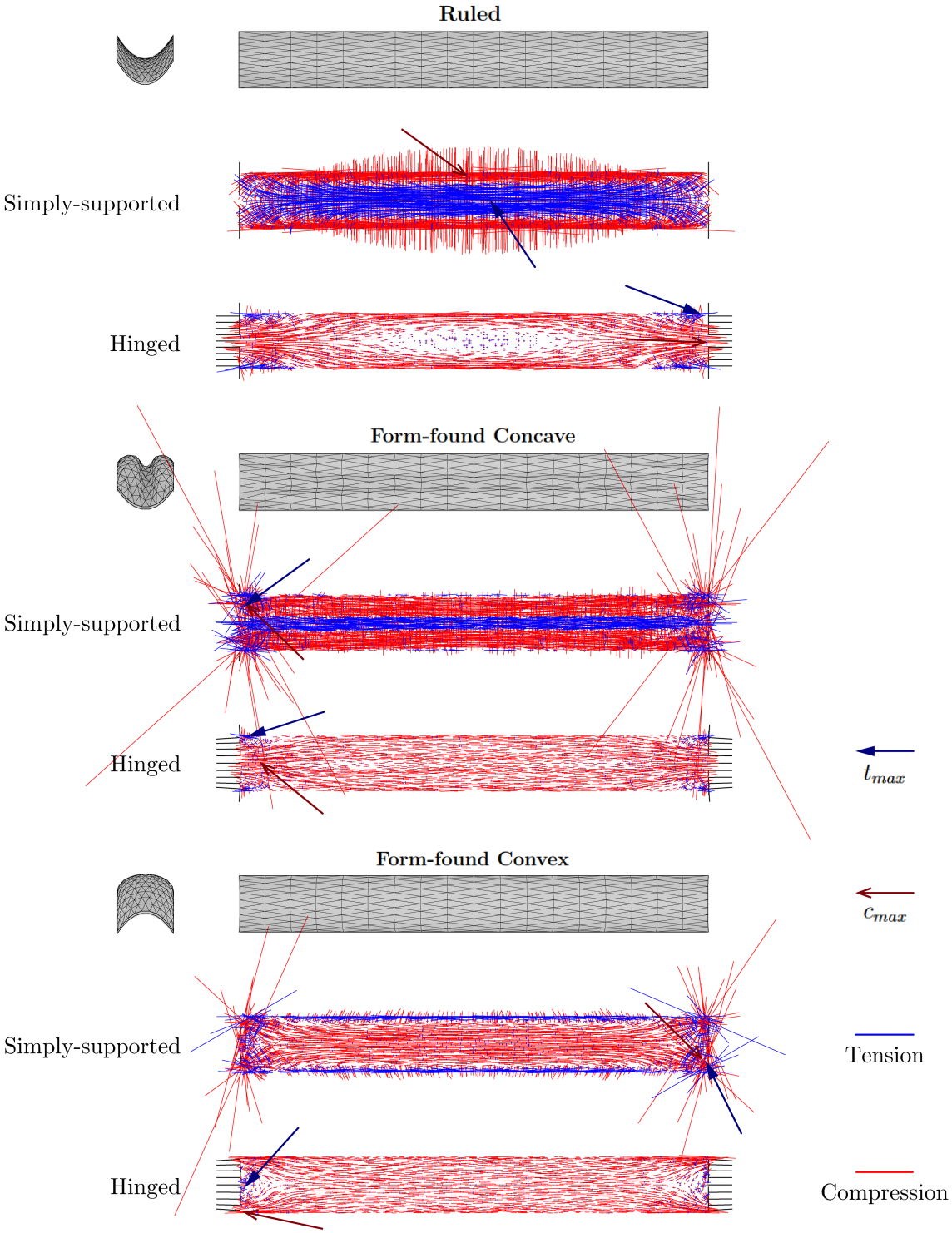

Figure 5.6: *Principal stress plots for the three slabs.*

Table 5.1: *Stresses σ [MPa] and maximum deformations $\delta_{\max}$ [mm] for the three slabs.*

		Hinged		**Simply-supported**	
		Whole	Half	Whole	Half
Ruled	$\sigma_{c,\max}$	-9.63	-9.01	-35.77	-31.64
	$\sigma_{t,\max}$	13.22	13.14	22.96	20.01
	σ_{centre}	0.78	0.66	22.96	20.01
	σ_{mid}	-7.02	-6.08	-29.6	-25.8
	$\delta_{\max}$	4.8672	4.23	47.13	41.144
Concave	$\sigma_{c,\max}$	-7.33	-7.63	-124.29	-103.44
	$\sigma_{t,\max}$	5.66	6.93	38.11	31.54
	σ_{centre}	-1.81	-1.75	12.89	2.95
	σ_{mid}	-2.34	-2.05	2.45	1.90
	$\delta_{\max}$	1.7534	2.106	42.228	35.1556
Convex	$\sigma_{c,\max}$	-11.64	-12.08	-177.36	-147.65
	$\sigma_{t,\max}$	1.67	2.46	33.38	27.78
	σ_{centre}	-2.26	-1.77	-6.53	-5.31
	σ_{mid}	-1.42	-1.42	-6.33 | 9.7*	7.77
	$\delta_{\max}$	1.8832	1.8089	21.2	17.5669

* For σ_{centre} and σ_{mid} there may be two present forces in different direction, one tensile and one compressive. $\sigma < |0.5|$ is left out. For σ_{mid} for the convex simply-supported with whole surface load, neither tensile or compressive was to small to neglect.

5.3 Discussion

From the principal stress plot (fig. 5.6), we can see that all the simply-supported slabs work as a simply-supported beam carrying loads through bending. There are big tensile stresses in the middle of the span. This is not ideal. By comparing table 5.1 to table 4.2 we can see that the compressive stresses can not be handled by even the highest class of concrete.

However, the hinged slabs perform well. We get compressive stresses that can almost be handled by the lowest concrete class for all the geometries. For a slab length of 10 m and a height of 1 m, we get a max deflection of 5 mm, which equals $L/2000$, to be compared to $L/300$, which is a commonly used deflection limit for slabs. The tensile stresses exceed the material capacity, requiring a mitigation of tensile stress through alteration of the geometry, or introduction of pre-stressing.

To enable implementation of prefabricated doubly-curved slabs, they need to be able to support their own weight without any supports when being transported and handled by cranes etc. The construction of a hinged support might also be difficult. When two slabs are meeting at a vertical support this is possible by having their horizontal forces counter each other, but the horizontal forces still needs to be taken care of at the end of the slab system. This is another problem that pre-stressing might solve, by making the slabs act as hinged internally but only transferring vertical loads to the supports.

5.3.1 Ruled surface

When examining the ruled surface, I found that the cross section in the yz-plane is identical for every x. This might be a big advantage when discussing production, since this enables a mold that can be reused and adapted to the desired slab length and height. This will be further discussed in section 8.2.1.

The linearity of the generatrices, also discussed by Osman-Letelier et al. (2019), is advantageous when exploring pre-stressing of the geometry. Having pre-stressed linear cables along the diagonals of the slab might make the simply-supported slab act as a hinged slab (as discussed in section 5.3), while also improving the performance of the slab.

5.3.2 Concave form-found surface

The concave form-found surface might be the geometry that is most affected by the approximation needed to allow simulation of the structural behaviour (see section 1.2). The second order of forces applied in the geometry generation (fig. 5.2c) gives the surface are varying depending of the mesh density. Figure 5.7 displays the different shapes depending on mesh density. The surprising fact is that even though the surface used in the model analysis differs from the most 'natural' shape, it still performs quite well. The biggest tensile stresses for the hinged concave slab is 6.93 MPa, which is smaller than the tensile stresses in the ruled surface. However, they are still to big to be handled by the concrete itself.

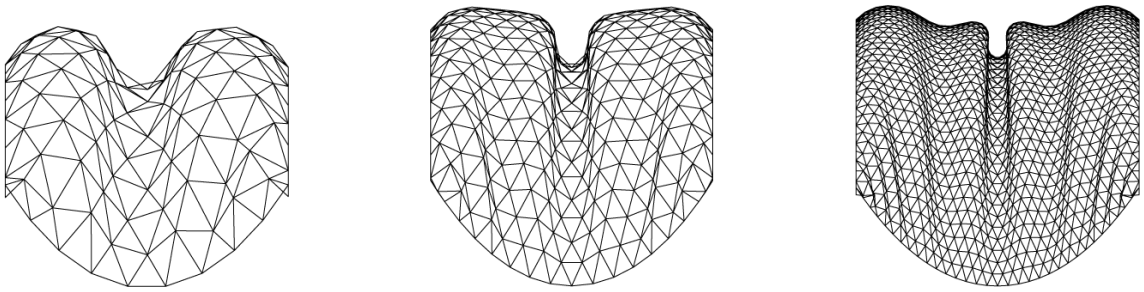

(a) $n = 342$ **(b)** $n = 1056$ **(c)** $n = 4160$

Figure 5.7: *Side view of the concave form-fond slab with the number of faces n.*

5.3.3 Convex form-found surface

The convex form-found surface is the geometry that as hinged produced the least tensile stresses in this study. They are so small that they just exceed the tensile stress of the concrete class C90/105. However, the pre-fabrication related issues discussed in section 5.3 still applies, requiring introduction of pre-stress to the slab.

6

Study II

Further adaptation and pre-stressing of the ruled surface slab

The aim of Study II is to explore whether simply-supported doubly-curved slab can be pre-stressed to make the principal stresses similar to the hinged versions from Study I.

As mentioned in section 5.3.1, the ruled surface is advantageous when discussing pre-stressing due to the straight generatrices along the surface. No internal straight lines could be found along the form-found surfaces, and they were therefor excluded from this study. The geometry used in Study II was the same as in Study I: 10 m long, 1.2 m wide, and 1 m high. The load combinations was kept the same, with the addition of pre-stress forces.

The study also tries to adjust the geometry and boundary conditions to better simulate the practical implementation of the slab. In Study I, the horizontal alignment was solved by filling the slab with gravel. For Study II, the option of lightweight fill (such as Leca) and very light fill (negligible weight) was also explored, to see how this affects the structural behaviour of the slab.

6.1 Method

This section discussed the method applied through support setup, pre-stressing and fill elaboration.

6.1.1 Support setup

Supposing that the slab will rest on supports with a flat top, the curved slab would need to be adapted to the supports to ensure stability.

As a first step in this study, the supported edges of the slab was extruded to a horizontal line, giving the slab a thickened edge—'shoes'—at the ends of the slab (fig. 6.1). The shoes also helps with mitigating the stress concentrations that can occur when introducing pre-stress. To simulate these shoes in the FE model, fictitious bars with large stiffness was added to the slab ends, see fig. 6.2 .

The linear supports used in Study I was replaced with point-supports, acting at the vertices of the slab edges. The supports was assigned only vertical strength, allowing all horizontal and rotational movements. The middle point for one of the edges was fixed horizontally to make the deformations relative to the slab itself.

Figure 6.1: *Ruled slab with thickened edges—'shoes'—to meet the external supports.*

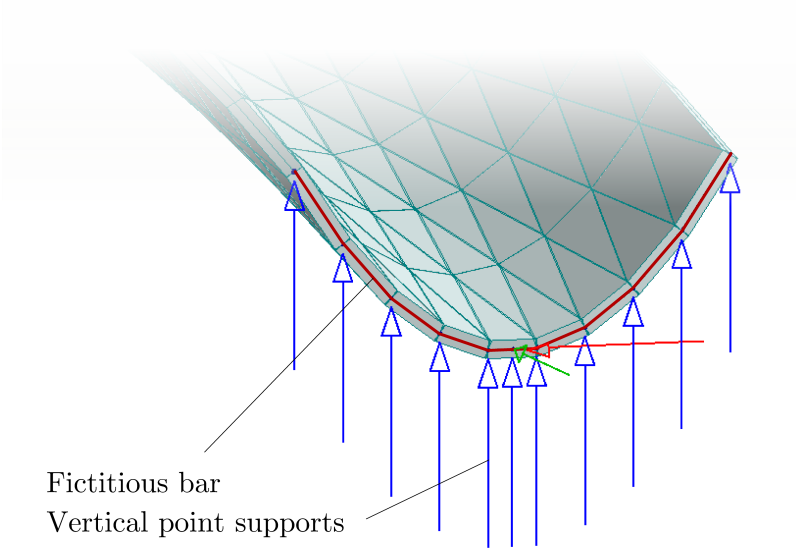

Figure 6.2: *Support setup used in Study II.*

6.1.2 Pre-stressing and fill elaboration

Next, two types of pre-stressing was added. The first pre-stressing layout was external, where three sets of strands were added between the shoes, parallel to the slab length. One strand between the centres of the shoes, and one at each side of the slab, see fig. 6.1. A pre-tension force of 100 kN was added over the middle bar. The resulting stresses over the slab with and without pre-stress were plotted.

The second type of pre-stressing included internal strands following the diagonal generatrices crossing in the middle of the slab, see fig. 6.4. Three different load cases were created, see table 6.1, where the three 15.7 mm radius strands were pre-stresses with the same amount. The resulting stresses is summed to 100, 150, and 300 kN. The results were plotted over the slab.

A final pre-stressing case was constructed, involving both the internal and external strands, see fig. 6.5. The stresses of the possible load combinations were plotted with a live load covering whole and half of the slab.

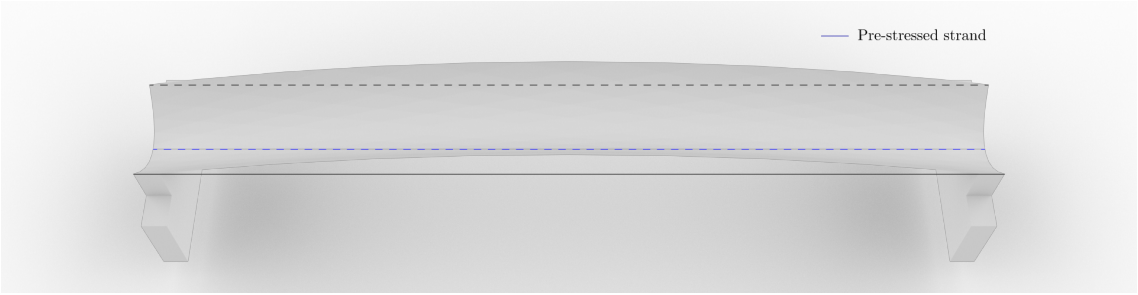

Figure 6.3: *Ruled slab with external strands.*

Table 6.1: *The three pre-stressing cases used for the internal strands.*

Pre-stress in one strand [MPa]	**Total pre-stress [MPa]**
33.3	100
50	150
100	300

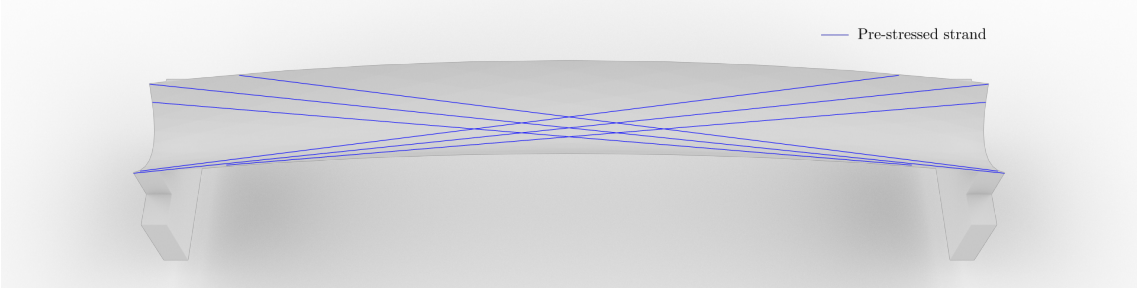

Figure 6.4: *Ruled slab with internal strands following the straight diagonal generatrices.*

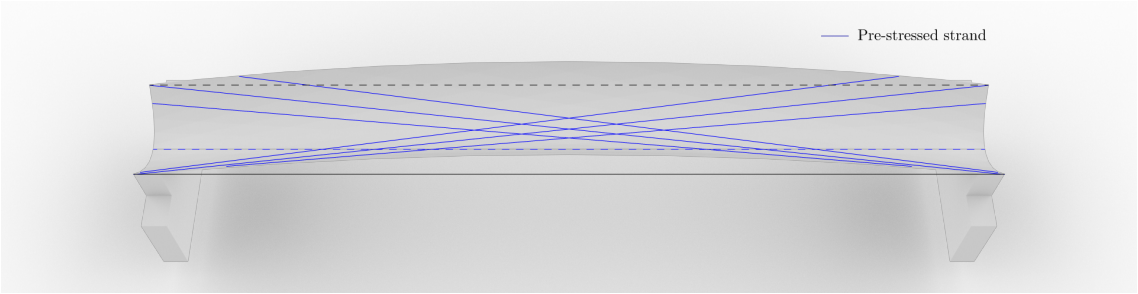

Figure 6.5: *Ruled slab with both internal and external strands*

The same pre-stressing cases were then simulated and plotted for three slabs, one where the gravel fill was replaced with lightweight fill and one where the fill was removed, see fig. 6.6. This was done to see how this affected the needs for pre-stressing.

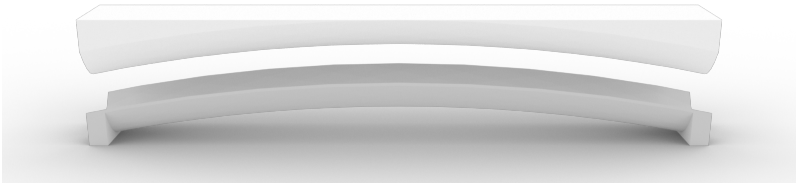

(a) *Gravel fill, ρ=1750 kg/m^3.*

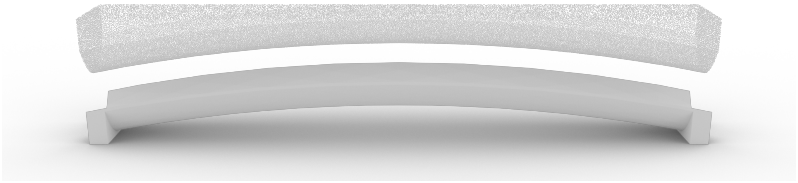

(b) *Lightweight fill, ρ=300 kg/m^3.*

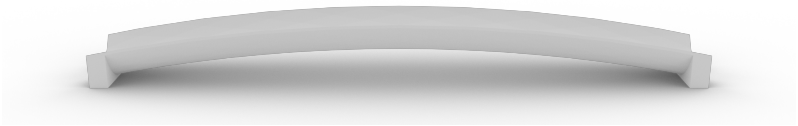

(c) *Unfilled, ρ=0 kg/m^3.*

Figure 6.6: *Ruled surface slab with the three different fills used in Study II.*

6.2 Results

This section includes the principal stress plots for the different pre-stressing cases. Each stress plot, figs. 6.7 to 6.17, displays the principal stresses and the maximum tensile stress $\sigma_{t,\max}$ and compressive stress $\sigma_{c,\max}$. To exclude fictive stress concentrations, the 5% highest absolute stresses are disregarded.

Table 6.2 shows the 36 load cases tested in this study, and which figure display the 11 cases deemed relevant.

Table 6.2: *Figure references for considered load cases and applied pre-tension force.*

		Figure reference					
		Gravel		Lightweight		Unfilled	
Pre-stressing case	Total tension [kN]	Whole	Half	Whole	Half	Whole	Half
External	0	6.7	-	-	-	-	-
	100	6.8	-	-	-	6.9	-
Internal	100	6.10	-	-	-	-	-
	150	-	-	-	-	-	-
	300	6.11	-	6.12	6.13	6.14	6.15
Both	100/300	6.16	6.17	-	-	-	-

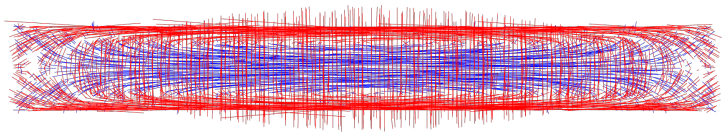

$\sigma_{t,\max} = 14.80$ MPa $\sigma_{c,\max} = -21.1$ MPa

Figure 6.7: *Gravel filled slab with untensioned external strands.*

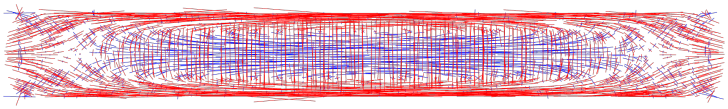

$\sigma_{t,\max} = 7.87$ MPa $\sigma_{c,\max} = -14.51$ MPa

Figure 6.8: *Gravel filled slab with 100 kN tensioned external strand, see fig. 6.3.*

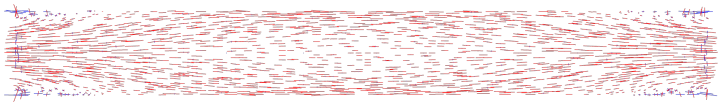

$\sigma_{t,\max} = 0.28$ MPa $\sigma_{c,\max} = -2.93$ MPa

Figure 6.9: *Unfilled slab with 100 kN tensioned external strand.*

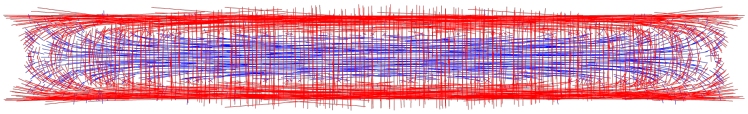

$\sigma_{t,\max} = 12.85$ MPa $\sigma_{c,\max} = -24.4$ MPa

Figure 6.10: *Gravel filled slab with 33 kN tensioned internal strands, see fig. 6.4.*

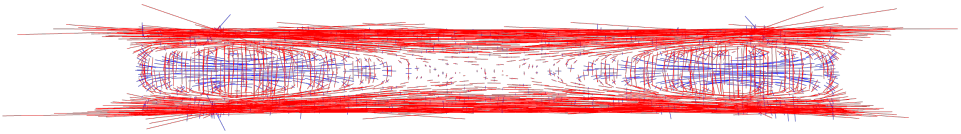

$\sigma_{t,\max} = 5.02$ MPa $\sigma_{c,\max} = -24.78$ MPa

Figure 6.11: *Gravel filled slab with 100 kN tensioned internal strands.*

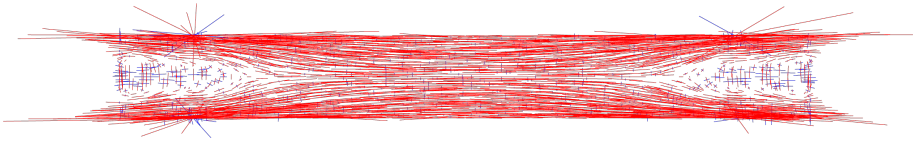

$\sigma_{t,\max} = 1.67$ MPa $\sigma_{c,\max} = -17.21$ MPa

Figure 6.12: *Lightweight filled slab with 100 kN tensioned internal strands.*

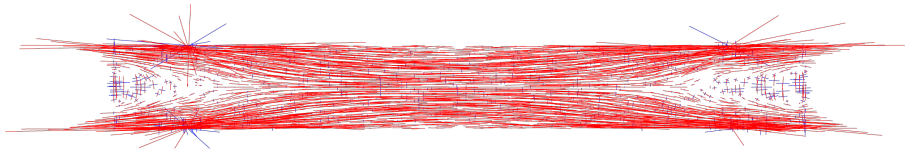

$\sigma_{t,\max} = 1.67$ MPa $\sigma_{c,\max} = -17.21$ MPa

Figure 6.13: *Lightweight filled slab with tensioned 100 kN internal strands under live load over half the slab.*

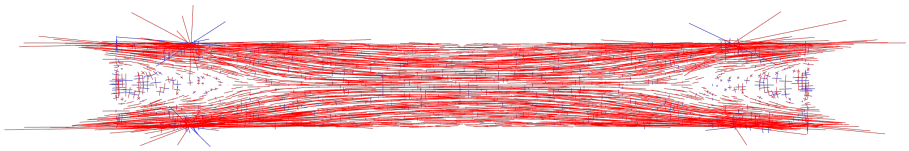

$\sigma_{t,\max} = 1.47$ MPa $\sigma_{c,\max} = -15.7$ MPa

Figure 6.14: *Unfilled slab with 100 kN tensioned internal strands.*

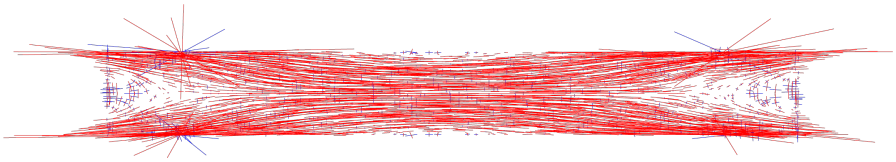

$\sigma_{t,\max} = 1.47$ MPa $\sigma_{c,\max} = -15.7$ MPa

Figure 6.15: *Unfilled slab with 100 kN tensioned internal strands under live load over half the slab.*

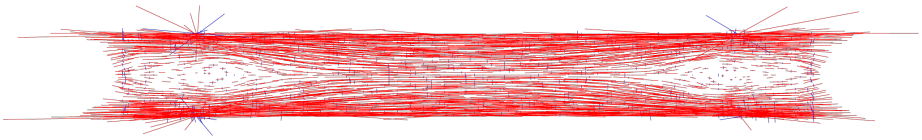

$\sigma_{t,\max} = 0.27$ MPa $\sigma_{c,\max} = -2.9$ MPa

Figure 6.16: *Gravel filled slab with 100 kN tensioned internal and external strands, see fig. 6.5.*

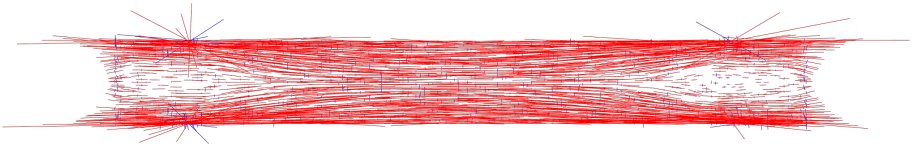

$\sigma_{t,\max} = 0.28$ MPa $\sigma_{c,\max} = -2.93$ MPa

Figure 6.17: *Gravel filled slab with tensioned internal and external strands under live load over half the slab.*

6.3 Discussion

The results from Study II shows it is possible to pre-stress a simply-supported ruled slab element to make it behave like a hinged element. We can also see that the maximum tensile stress, which is critical for concrete, is reduced for the pre-stressed slabs compared with the ruled hinged slab from Study I (see table 5.1).

By using the external pre-stress case, the smallest tensile forces in the slab are obtained. Since the tensile stresses are the critical for concrete, this pre-stress setup could be argued as beneficial. When studying older large-span stone buildings, we see the same method being used to mitigate the horizontal components of the outward thrust from slab-like arches. However, such designs lack redundancy, and are sensitive to temperature changes. If a fire would occur and heat up the steel strand, the tensile stiffness of the steel would be greatly reduced, and ultimately lose its purpose to keep the slab from snapping and releasing the slab ends outwards with an enormous force. This of course excludes the solution of using only regular steel in the strand, and would either require some other more heat-resistant material, or a heat protection treatment.

One large advantage of the internal pre-stressed strands is the linearity discussed earlier, especially in reference to slab production. The pre-stress of the strand could easily be mounted before casting of the concrete, without using special shape adjustment technique. The strands could simply be tensioned in-place. The covering concrete layer would protect the strands from direct heat in case of fire. The steel strands can still be subjected to corrosion and bond-slip, which needs to be taken into account during the design of the shell thickness.

Even if the pre-stressed slab is behaving like a hinged slab, the tensile stresses in the concrete are still to large to be handled by the material. To further develop the design to an applicable state, solutions to remove or mitigate these needs exploring.

None of the pre-stressed slabs exceeds the compressive strength of concrete (see section 4.3.1). An interesting note is that the slab with largest compression is not the one with the most pre-tension, but the gravel-filled 100 kN internally-tensioned (see fig. 6.11). I believe this is because the slab carries some of the forces through bending, like in a regular simply-supported beam. We get next to no compression in the middle of the transverse direction of the slab, which furthers points to this conclusion.

It is also clear that the lightweight fill results in smaller tensile forces than the gravel fill, while still fulfilling the requirement of simple installation and low climate impact. Because of this, the lightweight fill will be the considered fill in the following studies.

7

Study III

Structure elaboration to reduce tensile stresses

The main goal of Study III is to limit the tensile principal stresses in the slab enough for the concrete to not break. Two possible solutions are explored: thickening of the slab and elaboration with the boundary conditions. The minimum concrete cover required for the element is also calculated.

The aim of this thesis is to reduce the concrete usage. For the investigated slab element, its thickness is one of the main factors affecting this reduction. The thickness is decided by two main factors: if the material can handle the stresses it becomes subjected to, and the minimum concrete cover. The minimum concrete cover is defined to ensure:

- the safe transmission of bond forces between the concrete and reinforcement bars or stands,
- the protection of the steel against corrosion,
- an adequate fire resistance.

According to Eurocode 2 (2008), the minimum concrete cover is:

$$c_{\text{min}} = \max\{c_{\text{min,b}}; c_{\text{min,dur}} + \Delta c_{\text{dur},\gamma} - \Delta c_{\text{dur,st}} - \Delta c_{\text{dur,add}}; 10\ mm\} \tag{7.1}$$

where:

$c_{\text{min,b}}$	minimum cover due to bond requirement, equal to 2.5 times the diameter of indented pre-stressed strands,
$c_{\text{min,dur}}$	minimum cover due to environmental conditions,
$\Delta c_{\text{dur},\gamma}$	additive safety element, (recommended as 0)
$\Delta c_{\text{dur,st}}$	reduction of minimum cover for use of stainless steel, (recommended as 0)
$\Delta c_{\text{dur,add}}$	reduction of minimum cover for use of additional protection, (recommended as 0).

7.0.1 Thickening of the slab element

In Study II the shell thickness was 50 mm. As mentioned earlier, there are two factors deciding the element thickness. In the middle region of the span (x = 1.5–8.5 m), the 50 mm thickness was enough to handle the stresses for the internally pre-stressed lightweight-filled 10 m slab. The factor deciding the thickness in this

region will be the minimum concrete cover for the pre-tensioned strands. At the end regions of the span, ($x = 0$–1.5 m and $x = 8.5$–10 m) the tensile forces are too large to be handled by the concrete.

If the thickness of the concrete is locally increased at the end regions, these stresses might be lowered, while the amount of concrete in the slab could still could be kept low in comparison to the traditional slab systems.

7.0.2 Boundary condition elaboration

Another approach to reduce the tensile stresses is to further explore how the slab behave given other boundary conditions. How and where the slab wants to transfer out the horizontal stresses could show the solution for tensile stress reduction.

7.1 Method

The method section describe how the modelling and simulations are conducted for the thickening of the concrete layer and exploration of boundary conditions.

7.1.1 Thickening of the concrete layer

I started out Study III by finding the minimum concrete cover for the pre-stress strands in the resulting design from Study II. Cylindrical concrete bars with the radius of the strand (7.85 mm) plus this cover thickness was added along the strands. The resulting geometry was then simulated for the same load combinations and support setup used in Study II, see section 6.1.1.

The tensile forces were still to large for the concrete. To try and counter these, the thickness of the slab was increased at the areas where these acted. The concentration of tensile forces is shown in fig. 7.1. Three different thicknesses were setup to find how the thickness affected the behaviour of the slab, the original 50 mm with an addition of 50, 75, and 100 mm. The thickened slabs were simulated for the whole live load, lightweight fill, and simple supports used in Study II.

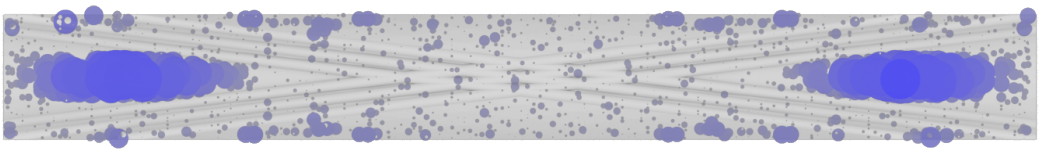

Figure 7.1: *Concentration of tensile forces. The darkness and diameter of each circle represents the stress magnitude at the centre of the circle.*

7.1.2 Exploration of boundary conditions

To not discard the option of a non-thickened slab, three other models were made. For all the models, the number of diagonal internal strands were increased from 3 per corner to 7, see fig. 7.2.

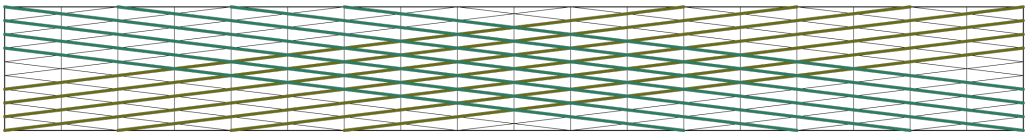

Figure 7.2: *Internal pre-stressing setup with 7 strands in each direction.*

The first model was based on the idea of letting the slab behave as it wants, under point supports acting at the ends of each strand, parallel to the strand, see fig. 7.3a. The z component of each support was removed to prevent the vertical loads to be taken out of the system anywhere but at the supports at the slab ends.

The second model was set up with point loads applied at the ends of each strand, parallel to the strand, see fig. 7.3b. Each point load was given a magnitude of 50 kN.

The third model included line loads applied along the pre-stress strands, with 50 kN of pre-stress over each strand, see fig. 7.3c. The results of each pre-stress setup was plotted for the whole live load, lightweight fill and simple supports used in Study II.

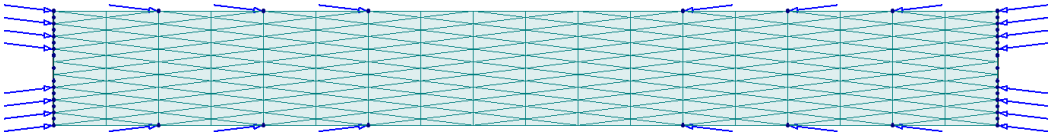

(a) *Point supports acting at the ends of the internal strands.*

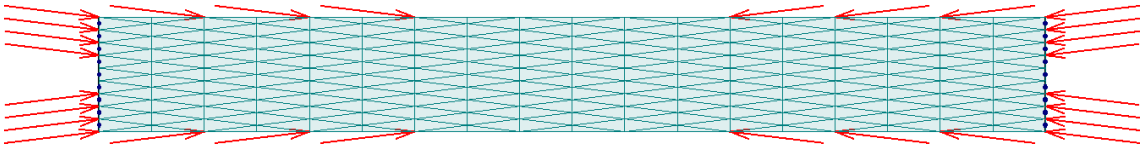

(b) *Point loads acting at the ends of the internal strands.*

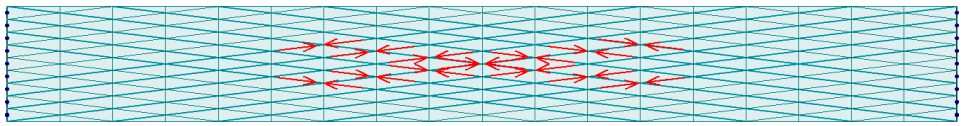

(c) *Line loads acting along the internal strands.*

Figure 7.3: *Boundary conditions to simulate pre-stress.*

7.2 Result

The results for Study III involves the thickened geometry and the corresponding principal stress plots, together with the principal stress plots for the new boundary conditions. The principal stresses for fig. 7.4 can be seen in figs. 7.5 to 7.7. Figures 7.8 to 7.11 are displaying stresses for the boundary conditions shown in figs. 7.3a to 7.3c. The 5% highest absolute stresses are disregarded.

7.2.1 Thickened element

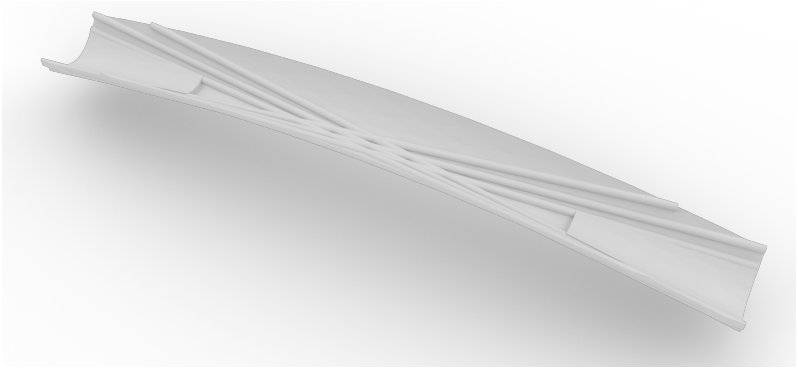

Figure 7.4: *Slab element with a thickened concrete layer around the strands and at the location of the tensile force concentrations.*

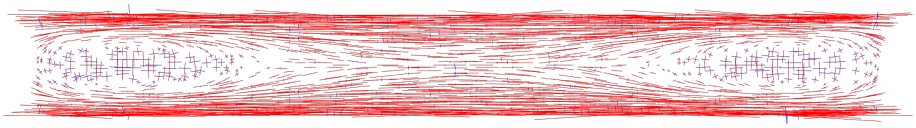

$\sigma_{t,\max} = 1.2$ MPa $\sigma_{c,\max} = -12.71$ MPa

Figure 7.5: *Principal stress plot for the slab element with thickened concrete layer around the strands.*

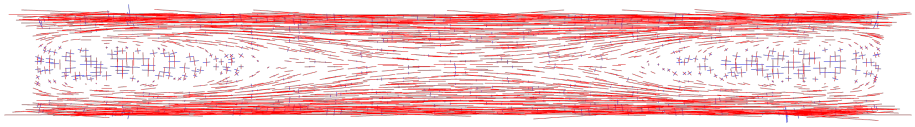

$\sigma_{t,\max} = 1.18$ MPa $\sigma_{c,\max} = -12.78$ MPa

Figure 7.6: *Principal stress plot for the slab element with thickened concrete layer around the strands and an addition of 5 cm at the location of the tensile force concentrations.*

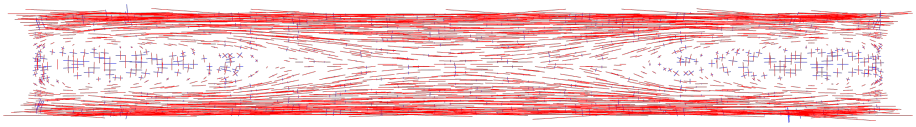

$\sigma_{t,\max} = 1.07$ MPa $\sigma_{c,\max} = -12.81$ MPa

Figure 7.7: *Principal stress plot for the slab element with thickened concrete layer around the strands and an addition of 10 cm at the location of the tensile force concentrations.*

7.2.2 New boundry conditions

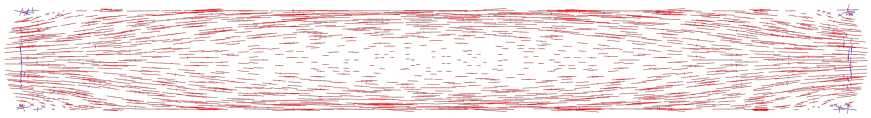

$\sigma_{t,\max} = 0.35$ MPa $\sigma_{c,\max} = -4.12$ MPa

Figure 7.8: *Principal stress plot for the non-thickened slab element with point supports applied at the ends of the internal strands.*

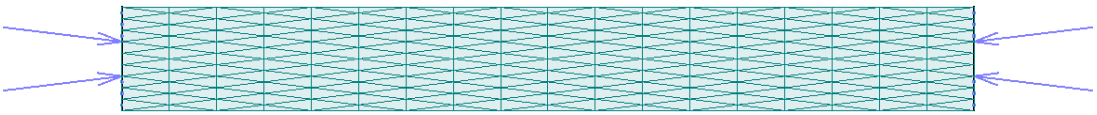

Figure 7.9: *Reaction forces in the point supports along the slab (compare with fig. 7.8).*

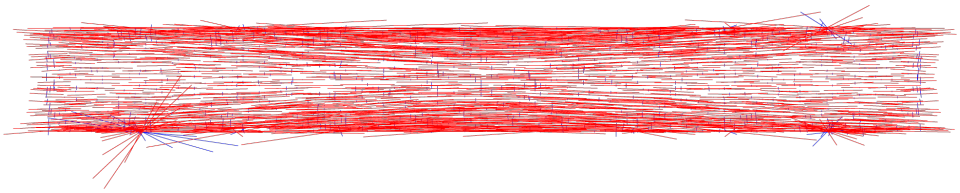

$\sigma_{t,\max} = 1.04$ MPa $\sigma_{c,\max} = -14.59$ MPa

Figure 7.10: *Principal stress plot for the non-thickened slab element with 50 kN point loads applied at the ends of the internal strands.*

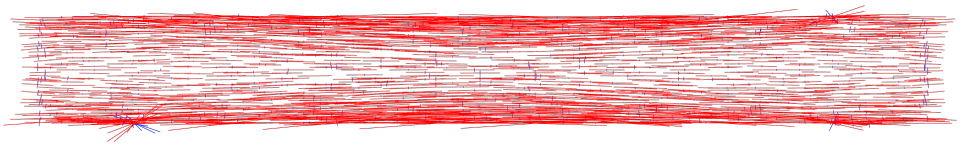

$\sigma_{t,\max} = 0.75$ MPa $\sigma_{c,\max} = -13.58$ MPa

Figure 7.11: *Principal stress plot for the non-thickened slab element with 50 kN line loads applied along the internal strands.*

7.3 Discussion

In this section the results of Study III is discussed, with the main focus being the impact of the methods to reduce tensile stresses.

7.3.1 Thickened element

Since the stress is defined as force per area, the initial idea of Study III was to see if the cross-sectional area of the slab could be increased locally to limit the tensile stresses in the slab. The increased thickness was also required to fulfill the minimum concrete cover demanded by EC 2 for the strands used in Study II. The results of this simulation was quite unsatisfactory however. By comparing figs. 7.5 to 7.7, it is clear that an increased cross-sectional area does not result in a significant reduction of stresses. The tensile stresses are reduced marginally, and the compressive forces are increased by a similar amount.

The local slab thickening is, however, increasing the complexity of the production process. The made up production method, discussed in the following study, is built around the identical cross section of the ruled surface. If the thickness is increased locally, the cross section is altered depending on where in the span we are looking. The solution to apply the thicker parts afterwards can be discarded due to the in-homogeneous hardening for the element, which would compromise the slab behaviour.

The solution to increase the thickness of the entire slab to make the cross section identical to the most thick cross section would make the entire slab element system useless, since the idea of the system is to reduce the material use.

7.3.2 New boundry conditions

The main goal of the model with supports along the slab was to see how the element wanted to behave, provided the possibility of mitigating outwards facing stresses through the point supports. The idea was that if given the possibility, the structural behavior would limit the internal tensile stresses through mitigation, similar to the form-found geometries discussed in section 4.1.2 and Study I. By studying fig. 7.8 the method is clearly working to limit all the stresses in the slab element. The only points taking significant loads are the two most central at the slab edges, as seen in fig. 7.9. The explanation for this is that in order to balance the internal forces, the slab simply acts as a doubly-curved arch. This further explains why the external pre-stressing cases in Study II were so successful (see section 6.3).

However, as discussed in Studies I and III, the possibility to mitigate the stresses on the outside of each slab element counteracts the goal to make the slab element work on its own. If the slab element can manage the stresses internally, without external strands or horizontal stiffening, this is preferred. The external current supporting structures would not need altering to make the internally pre-stressed slab system work.

On the other hand, both the point loaded and line loaded models perform well. All the internal tensile stresses are surpassed by the concrete tensile strength. The compressive stresses are also small enough to be handled by the concrete classes 25/30 and above. The lower pre-stress forces required for each strand (resulting from the increased number of strands), also allow thinner strands which require a smaller minimum concrete cover. For a stress of 50 kN, the diameter does not have to exceed 6 mm. This lead to an element thickness of less than 40 mm. A preliminary evaluation of the thinner element shows that this thickness is also handling the forces.

The thinner strands also mean that the thickness of the slab can be uniform over the element, resulting in a much simpler production process. The concrete could simply be poured over the straight pre-stressed strands in the adaptable form discussed in section 5.3.1.

Whether all the strands need pre-stress, or if some of them can be replaced with simple straight reinforcement bars is something for another study. This would result in a lower production cost.

8

Study IV

Production and climate impact

Study IV revolves around evaluating the first implementation related issues and questions for the resulting slab element from Study III. Unlike the earlier studies, this study does not involve stress simulations, but has a more conclusive approach.

8.1 Method

This section begins with the thought production of the slab element, and continues to discuss the climate impact that it might have. The climate impact is compared to other concrete pre-fabricated slab systems that are common today.

8.1.1 Production method

Studying existing production methods for modular doubly-curved concrete elements, like the Adapa adaptive moulds (see fig. 8.1) (Adapa A/S, 2022), a concept for rational production of the ruled slab element was constructed. The method was based on the identical cross section along the ruled slab element, briefly discussed in section 5.3.1.

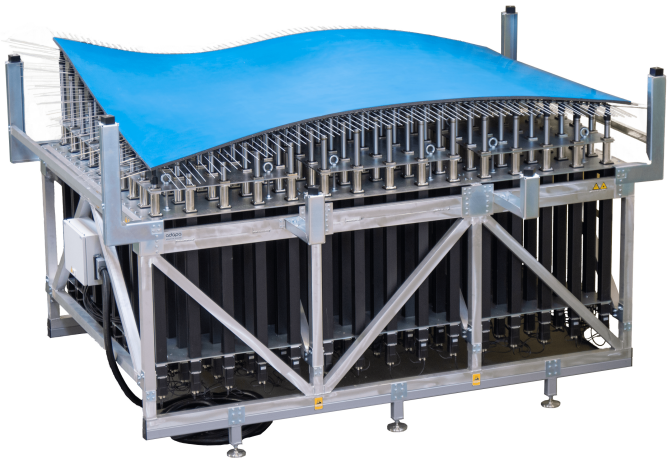

Figure 8.1: *Adaptive piston controlled concrete mould. Photo credit: Adapa A/S.*

8.1.2 Climate impact

To roughly estimate the climate impact of the doubly-curved shell-like slab, the CO_2e/kg for the life-cycle phases A1-A3 was calculated for the resulting line-stressed 40 mm thick slab from Study III. This was done using the climate database provided by Boverket (2023). The CO_2e/kg for TT slabs and hollow core slabs was taken from the same database. The CO_2e/kg was then converted to CO_2 equivalents per square meter for the selected slab elements.

Some parameters from currently used systems was found, and these were compared to the ruled slab to get an as similar as possible system to compare with. The parameters were centred around the system geometry and structural efficiency. The parameters were:

- Height,
- length dependency,
- cross-sectional area,
- load capacity.

A master thesis evaluating these parameters is written by Högström and Olsson (2001). In the thesis, three pre-fabricated slab systems are presented, hollow core slabs, TT slabs and lightweight concrete elements.

8.2 Results

This section discribe the thought of production process, and the calculation of the material climate impact of the ruled slab, hollow core slab and TT slab

8.2.1 Production method

The thought rational production method looks as following:

Step 1 (fig. 8.2a): Identical thin (1-5 cm) plates are stacked next to each other. Since the width of the element is standardized to 1200 mm (see section 1.2), the plates can be mass produced and reused. The curvature in each plate varies for different slab element lengths, but this thesis will not dive deeper into this matter.

Step 2 (fig. 8.2b): The plates are adjusted vertically by pushing up the plates, using hydraulics, wedges or blocks. The plates are then fastened into place to handle the weight of the concrete.

Step 3 (fig. 8.2c): A semi-stiff rubber membrane or similar is placed in the plate form, to remove the small steps in the form and make the surface smooth. The pre-stress strands are put into place and tensioned. This is possible to do before the pouring of concrete due to the straight nature of the generatrices (see section 6.3). The concrete is then poured into the form over the strands. Other concrete application methods could be possible, such as spraying of the concrete.

Step 4 (fig. 8.2d): The concrete is left to harden, and the element is then removed from the form which can be used again. The excess pre-stress strands are cut away, leaving the thin doubly-curved shell-like slab element. The shoes (see section 6.1.1) are then added, and the element is ready for transportation and mounting at the construction site.

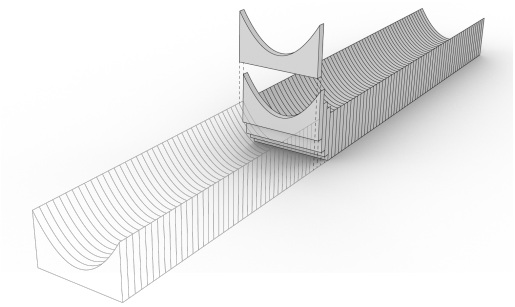

(a) *Step 1: Plate placement.*

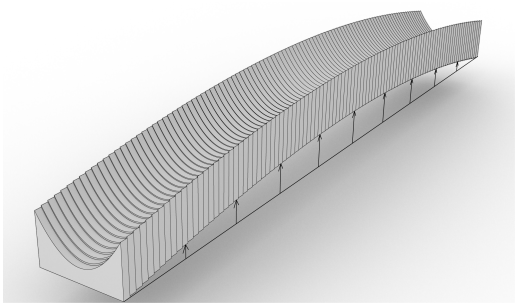

(b) *Step 2: Plate adjustment*

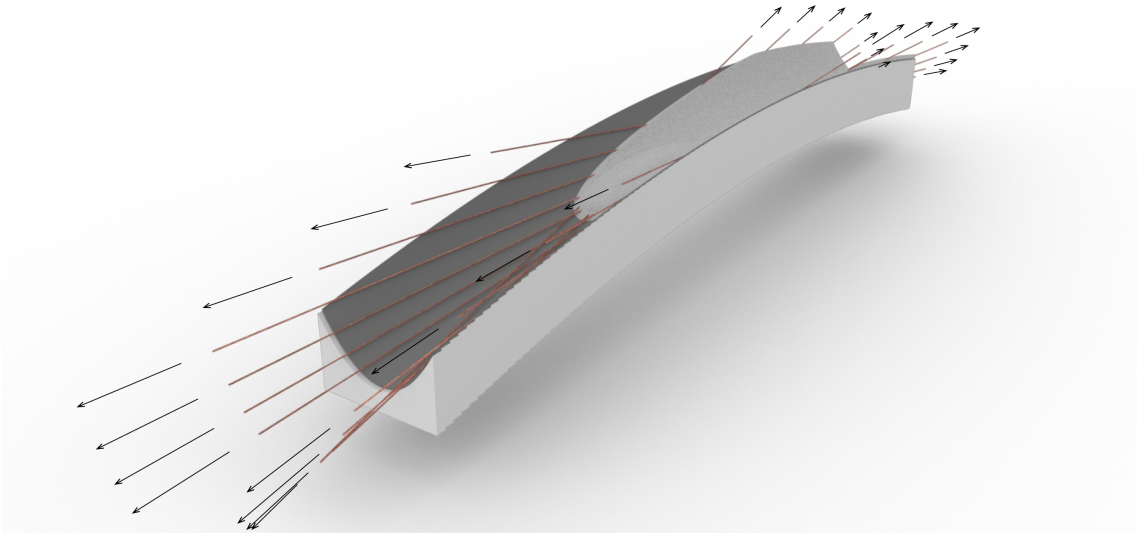

(c) *Step 3: Rubber membrane, pre-stress strands and concrete pouring.*

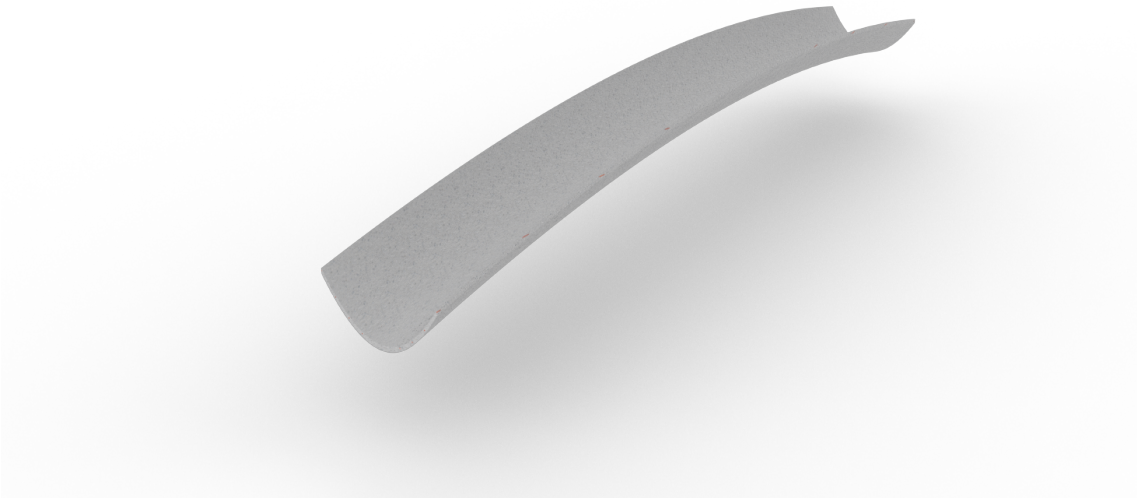

(d) *Step 4: Removal of hardened element from form, cutting of pre-stress strands.*

Figure 8.2: *The 4 steps of the thought production method.*

When the slab elements are placed on site, the are stacked next to each other in the same way as pre-fabricated slab systems used today, on top of a primary supporting structure. Piping and installations can then be placed in the slab system if desired. The slab system is then filled with lightweight fill, which can also include sound isolating material, to level. On top of the fill, the floor is placed.

8.2.2 Climate impact

Table 8.1: *Calculation of kg CO_2 equivalents per square meter for the ruled slab.*

	Concrete, class 25/30	Reinforcement strands
CO_2e/kg [kg]	0.129	1.25
volume [m^3]	0.467	0.0129
density [kg/m^3]	2500	7850
weight [kg]	1167.5	101.27
weight/m^2 [kg/m^2]	97.29	8.44
CO_2e [kg]	150.6	126.59
CO_2e/m^2 [kg]	12.55	10.55
Total CO_2e/m^2	**23.1 kg**	

The selected slab elements that best matched the ruled line- stressed 40 mm thick slab from Study III was hollow core slab HD/F 120/19 and TT slab TT/F 240/30.

Table 8.2: *Calculation of kg CO_2 equivalents per square meter for the hollow core and TT slabs.*

	hollow core slab 120/19	TT slab 240/30
CO_2e/kg [kg]	0.188	0.274
weight/m^2 [kg/m^2]	403.8	381.4
Total CO_2e/m^2	**75.91 kg**	**104.50 kg**

8.3 Discussion

I believe that the production method described is both rational and realistic. However, when comparing the efficiency of the production method with the hollow core or TT slabs, it has some weaknesses. The production of the hollow core and TT slabs is done by extruding concrete in a long form. The slabs are then cut to the right length, resulting in multiple slabs for each casting. The casting machine is programmable, and very little alterations of the cast are required depending on the specific slab type (i.e. 120/19, 120/27 etc.). This means that the production of these slabs is more effective than the ruled-slab production. The hollow core and TT slabs also require less pre-stress, which further simplifies the production in comparison.

When comparing the climate impact of the material use for the ruled slab with the hollow core and TT slabs, the reduction of the ruled slab becomes clear. The

75.91 and 104.50 kg CO_2e/m^2 for the hollow core and TT slab, compared with the 23.1 kg CO_2e/m^2 of the ruled, shows that even though the ruled slab contains more steel as a result of the larger required pre-stress, the ruled slab has less than a third the material climate impact compared with the conventional slabs. More precisely, the ruled slab has a climate impact 30% of the hollow core, and 22% of the TT slab.

9
Summary and Conclusion

This chapters begins with a summary and discussions of the results and conclusions of studies I-IV. It then continues linking back to the thesis aim, hypothesis and objectives. The chapter ends with suggestions for further research.

9.1 Summary

This section sum the results and conclusion of each study.

9.1.1 Study I

Study I revolved around two support types, and the difference between the ruled slab element and two form-found elements.

The simulations done in the study shows that non of the slabs function when only simply-supported. The stresses that occur in the slab is however much smaller for the hinged support, even though the tensile stresses are still a little too large to be handled by the material. The hinged supports also resulted in very small deformations, at around $L/2000$.

Some characteristics of the different element geometries were discovered during Study I. By the geometrical definition of the ruled surface, for each point in the surface there are two straight lines running between the edges of the slab, intersecting at the point. The cross-section of the ruled surface was also found to be identical, no matter where along the span it is taken.

9.1.2 Study II

In study II the possibility to replicate the hinged slab behavior for a simply-supported slab by using pre-stress was explored. For fire safety reasons, only internally pre-stressed slabs were deemed valid, and since none of the form-found slabs included any internal straight lines, these were discarded. Some further geometry elaboration was also done, through the addition of "shoes" at the slab ends, to promote element stability for flat topped supporting structures. Three different fills were also explored.

The results of Study II showed that the hinged behaviour was possible to replicate, by letting three 15.7 mm radius straight pre-stress strands run along the diagonals of the ruled slab. The addition of shoes further improved the slab performance, by mitigating stress concentrations at the slab ends. The replacement

of gravel (ρ=1750 kg/m^3) with lightweight fill (ρ=300 kg/m^3) was found beneficial, even under live load over only half the slab element.

9.1.3 Study III

The goal of Study III was to further limit the tensile stresses in the concrete to a level where the material would not crack. This was explored by two approaches, the first one being: *Thickening of the concrete layer*, and the second: *Exploration of boundary conditions*.

The concrete thickening was done by first evaluating the minimum concrete cover around the pre-stress main tensile stresses occurred close to the slab ends, in the middle of the transverse direction. Three different thicknesses were simulated, with a very small difference in results. The tensile stresses are reduced marginally with the increased thickness, but not enough to consider increased thickness as a solution for reduction of tensile stress.

For the second approach, additional boundary conditions along the slab edges, with supports taking loads parallel to the generatrices. The results of the simulation show that the horizontal behavior of the slab is to transfer all of the horizontal stresses out of the system at the middle of the slab ends. Since only internal pre-stress was allowed, the boundary conditions were hard to replicate in a optimal way. The solution decided was to add four more pre-stress strands per diagonal of the slab, resulting in 14 strands total. The result of the new pre-stress setup limited the tensile stresses to 0.75 MPa, which is within the concrete strength. The increased amount of pre-stress strands allowed for thinner pre strands, resulting in no requirement of extra concrete around these.

9.1.4 Study IV

In the and last study, the resulting design of Study III was evaluated. A production method was formulated, and the material climate impact was calculated and compared with two conventional slabs.

The production method discussed is based on modular reusable plates, that due to the fixed slab width can be reused again and again to eliminate construction and tear down of complex forms. The top shape of the plate might have to be adjustable, but that is something for future research.

The material climate impact showed that the thin ruled doubly-curved surface has has 22-30% the material impact of the conventional hollow core and TT slabs.

9.2 Aim, hypothesis and objectives

This thesis aims to discuss the possibility to lower the material climate impact of the construction industry, by changing the geometry of conventional slab elements to a doubly-curved shell-like geometry. The slab element designed in the thesis can replace traditional slabs, without further alteration of primary supporting structures. Another possible application of the element is in bridges. The aim and hypothesis

of the thesis is explored through the 4 studies, by geometry elaboration, evaluation and pre-stressing of the element.

9.2.1 First objective

The first objective was: *To explore and describe design choices that affects the structural efficiency in concrete slabs.* The thesis evaluate some design choices and the impact on the structural efficiency. In Study I, the form-finding design method was proved very beneficial in creating efficient geometry that distribute stress evenly. However, their non-linearity was in Study II ultimately found fatal. Study I show the support type dependency of the form-finding approach. In order to make the design method work, the supports used to find the geometry need to be identical to the supports that will support the standing structure.

The choices that affect structural efficiency are infinite in number. There is no possibility to cover them all, but this thesis grasp on a few of them.

9.2.2 Second objective

The second objective was: *To design and evaluate a doubly-curved slab element, to a point where it is theoretically implementable.* The resulting geometry (see fig. 8.2d) of this thesis work in theory. It is construable and applicable in present load-bearing systems. Therefor this objective is fulfilled. The practical production and stress testing of a pre-stressed ruled slab could be a next step in the implementation process.

9.2.3 Third objective

The third and last objective was: *To compare the resulting design with currently used systems, to see if the new slab element can reduce the climate impact.* The resulting 70-78% climate reduction is a satisfying conclusion to this objective.

9.3 Future Research

Like with most research, I feel that I have been giving rise to more questions than answers during the thesis. Some of the topics that need further investigation will be discussed in this section.

9.3.1 Further shape elaboration

To fully understand the possibilities and limitations of the ruled slab, further investigation of the shape is required. This thesis only study a 10 m long and 1.2 m wide slab elements. Different spans need to be further explored, and how the slab height impact the structural behaviour and material use. Another question regarding structural behavior is drilling through the element to make way for installations of ventilation, plumbing etc.

The behaviour of a slab system is also in need of evaluation, where the interaction of the elements, fill and load distribution is regarded. The possibility to use the fill volume, i.e. for sound insulation or horizontal installations, together with the spacial impact of the doubly-curved geometry could also impact the possibilities greatly.

9.3.2 Logistics and Production

The logistics and production optimization is only briefly touched upon in this thesis. This is a field that need more research. The transportation of the ruled slab needs further development. Both with cranes and trucks to the construction site, but also practical storage and installation at site. The plate setup discussed in section 8.2.1 needs further refinement in order to work for different lengths and heights.

9.3.3 Economic optimization and gains

The reduction in material use could be a great opportunity when discussing the cost of the slab, but needs to be weighted against the cost of production and transportation etc. In order to make the construction sector fully implement the slab, there needs to be an economical gain, which needs to be developed for the ruled slab. Further cost optimizations could include but not be limited to: replacing some of the pre-stress strands with regular reinforcement, cheap or multipurpose filling or increased number of slabs per truck due to less weight.

References

Adapa A/S. (2022). *Adapa adaptive moulds.* https://adapamoulds.com/. (Accessed: 2023-06-15)

Boverket. (2023). *Boverkets klimatdatabas* [database]. Retrieved from https://www.boverket.se/sv/klimatdeklaration/klimatdatabas/klimatdatabas/

Dombrowski, M., Merz, P., Osman-Letelier, J. P., & Schlaich, M. (2021). Transverse structural behaviour of doubly curved beam-like shells. In *Inspiring the next generation.* Guilford, UK.

Elliot, K. S. (2017). *Modernisation, mechanisation and industrialisation of concrete structures* (K. S. Elliot & Z. A. Hamid, Eds.). ohn Wiley & Sons, Incorporated.

European Commission. (2023). *Eurocodes: Building the future.* Retrieved from https://eurocodes.jrc.ec.europa.eu/

Foraboschi, P., Mercanzin, M., & Trabucco, D. (2014). Sustainable structural design of tall buildings based on embodied energy. *Energy and Buildings*, *68*(PARTA), 254-269 - 269. Retrieved from https://search.ebscohost.com/login.aspx?direct=true&db=edselc&AN=edselc.2-52.0-84887036085&site=eds-live&scope=site&authtype=guest&custid=s3911979&groupid=main&profile=eds

GlobalABC, IEA, & UNEP. (2020). *Globalabc roadmap for buildings and construction 2020-2050, towards a zero-emission, efficient, and resilient building and construction sector* (Report). Retrieved from https://globalabc.org/resources/flagship-products

Högström, R., & Olsson, T. (2001). *Betongbjälklag* (mathesis). Karlstads Universitet.

IEA. (2022a). *Building envelopes* (Report). Retrieved from https://www.iea.org/reports/building-envelopes

IEA. (2022b). *Cement* (Report). Retrieved from https://www.iea.org/reports/cement

Jaillon, L., Poon, C., & Chiang, Y. (2009). Quantifying the waste reduction potential of using prefabrication in building construction in hong kong. *Waste Management*, *29*(1), 309-320. Retrieved from https://www.sciencedirect.com/science/article/pii/S0956053X08000718

Martines, G. (2015). *The pantheon: From antiquity to the present* (T. A. Marder & M. W. Jones, Eds.). Cambridge University Press. doi: 10.1017/CBO9781139015974

Ochsendorf, J., & Block, P. (2014). *Shell structures for architecture: form finding and optimization* (S. Adriaenssens, P. Block, D. Veenedaal, & C. Williams, Eds.). London: Taylor & Francis - Routledge. Retrieved

from https://search.ebscohost.com/login.aspx?direct=true&db=cat09075a&AN=clpc.oai.edge.chalmers.folio.ebsco.com.fs00001000.b97d6850.570f.43f3.a017.8c034312667b&site=eds-live&scope=site&authtype=guest&custid=s3911979&groupid=main&profile=eds

Osman-Letelier, J. P., Lehrecke, J., & Schlaich, M. (2019). Structural optimization of prestressed concrete shells with ruled surface geometry. In C. Lázaro, K.-U. Bletzinger, & E. Oñate (Eds.), *Form and force 2019* (pp. 2622–2629). Barcelona, Spain: International Centre for Numerical Methods in Engineering (CIMNE).

Piker, D. (2017). *Kangaroo2* [software]. Retrieved from https://www.food4rhino.com/en/app/kangaroo-physics

Robert McNeel & Associates. (2022). *Grasshopper* [software]. Retrieved from https://www.grasshopper3d.com/

Sehlström, A. (2021). *Prestress and its application to shell, fabric, and cable net structures* (Doctoral dissertation, Chalmers University of Technology). Retrieved from https://search.ebscohost.com/login.aspx?direct=true&db=ir01624a&AN=crp.24825f69.ba01.4248.98a8.4674ac70bf03&site=eds-live&scope=site&authtype=guest&custid=s3911979&groupid=main&profile=eds

Strusoft. (2023a). *Fem-design 3d structure 22* [software]. Retrieved from https://strusoft.com/software/3d-structural-analysis-software-fem-design/

Strusoft. (2023b). *Fem-design api toolbox* [software]. Retrieved from https://www.food4rhino.com/en/app/fem-design-api-toolbox

Svensk betong. (2015). *Håldäck (hd/f).* https://www.svenskbetong.se/bygga-med-betong/bygga-med-prefab/statik/haldack. (Accessed: 2023-01-31)

Swedish Standards Institute. (2008). *Eurocode 2: Design of concrete structures - part 1-1: General rules and rules for buildings* (1st ed.).

Swedish Standards institute. (2013). *Swedish standard ss 212553:2013* [standard].

Timoshenko, S., & Goodier, J. (1951). *Theory of elasticity.* McGraw-Hill book company.

United Nations Environment Programme. (2022). *2022 global status report for buildings and construction: toward a zero-emissions, efficient and resilient buildings and constructions sector* (Report). Nairobi: United Nations Environment Programme.

Williams, C. (2014). *Shell structures for architecture: form finding and optimization* (S. Adriaenssens, P. Block, D. Veenedaal, & C. Williams, Eds.). London: Taylor & Francis - Routledge. Retrieved from https://search.ebscohost.com/login.aspx?direct=true&db=cat09075a&AN=clpc.oai.edge.chalmers.folio.ebsco.com.fs00001000.b97d6850.570f.43f3.a017.8c034312667b&site=eds-live&scope=site&authtype=guest&custid=s3911979&groupid=main&profile=eds